Validation of the Repurposing of the Methotrexate Scaffold for the Design of Janus Kinase Modulators with Potential Inhibitory Activity

Submitted in partial fulfilment of the requirements

of the Degree of Master of Pharmacy

Francesca Borg

Department of Pharmacy

2021

L-Università ta' Malta

University of Malta Library – Electronic Thesis & Dissertations (ETD) Repository

The copyright of this thesis/dissertation belongs to the author. The author's rights in respect of this work are as defined by the Copyright Act (Chapter 415) of the Laws of Malta or as modified by any successive legislation.

Users may access this full-text thesis/dissertation and can make use of the information contained in accordance with the Copyright Act provided that the author must be properly acknowledged. Further distribution or reproduction in any format is prohibited without the prior permission of the copyright holder.

Dedicated to my family and friends.

Abstract

Polycythaemia vera, a rare blood cancer, has been associated with a mutation in the *JAK2V617F* gene, in turn leading to the activation of the JAK/STAT signalling pathway. This receptor is therefore a target in the identification of molecules that target myeloproliferative neoplasms. Antagonism can reverse underlying marrow pathologies, disrupting erythrocytosis and other inflammatory responses. The identification of low-dose methotrexate as a selective and potent JAK2 antagonist indicates, that there is potential for its repurposing, since current treatments are associated with the increased risk of transformation of polycythaemia vera to acute leukemia. This study uses the methotrexate scaffold as the lead molecule in order to recognize high affinity ligands using two different approaches: virtual screening and *de novo* techniques. Conformational analysis was performed on the methotrexate scaffold. The methotrexate molecule was modelled and docked into the *apo* JAK2 receptor. This process generated 20 different conformers. The optimal conformer was identified by calculating the ligand binding energy in $kcalmol^{-1}$ and the ligand binding affinity in pKd for each conformer, and plotting them on a line graph. The molecule that was the most energetically feasible and that had the highest affinity was chosen as the best optimal conformer. In the Virtual Screening approach, the methotrexate molecule was used as the template to generate a cohort of Lipinski Rule compliant hit molecules. These hits were docked into a generated protomol and the resultant 991 compliant molecules were ranked according to their affinity for the JAK2 ligand binding pocket. In the *de novo* approach 3 seed structures were modelled, based on the optimal methotrexate molecule, and growth was allowed, through a fragmentation exercise, within the pharmacophoric space, in order to generate novel molecules. A number of filters were applied to ensure that the best molecules are Lipinski Rule compliant, and hence able to penetrate the blood brain barrier. Lipinski

Rule compliant *de novo* molecules were generated and separated into different families based on their pharmacophoric similarities, and then ranked according to affinity. The optimal molecules obtained from these two approaches will be retained for further validation and optimization.

Acknowledgements

I would like to express my heartfelt gratitude toward my supervisor, Dr Claire Shoemake, of the Pharmacy Department, for her continuous support and guidance throughout these five years.

I would also like to extend my thanks to the Head of Department Prof. Lillian Azzopardi and Prof. Anthony Serracino Inglott and all the staff at the Pharmacy Department for their professional help throughout the years.

Finally, I would like to thank my parents, my siblings Nicole and Kirstie, and the pharmacists and staff at Brown's Pharmacy Haz-Zebbug for their patience and support.

Table of Contents

List of Tables ……. ix

List of Figures …… x

List of Graphs …… xii

List of Appendices …… xiii

Glossary …… xiv

List of Abbreviations …… xv

1. Introduction …… 1
   1.1. Polycythaemia Vera …… 2
      1.1.1. Brief Overview …… 2
      1.1.2. Diagnosis and Prognosis …… 3
      1.1.3. Gene Expression …… 4
      1.1.4. Haematopoietic Stem Cell Bone Marrow Niches …… 5
      1.1.5. Current Treatment …… 6
   1.2. JAK2 …… 11
      1.2.1. Overview …… 11
      1.2.2. Mode of Action …… 13
      1.2.3. JAK2 Ligand Binding Pocket …… 14
      1.2.4. Endogenous Agonism of JAK2 …… 17
      1.2.5. JAK2 Inhibitors …… 17
   1.3. Methotrexate …… 19
      1.3.1. Overview …… 19
      1.3.2. Traditional uses of Methotrexate …… 22
   1.4. Drug Repurposing …… 23
      1.4.1. Overview …… 23
      1.4.2. Advantages of Drug Repurposing …… 24
      1.4.3. Disadvantages of Drug Repurposing …… 26
   1.5. *In silico* Techniques …… 26
      1.5.1. Computational Drug Design …… 26
      1.5.2. Software …… 28
   1.6. Aims …… 30

2. Methodology ……..…….…… 31
2.1. Introduction …….….. 32
2.2. Protein Data Bank Depositions ……..… 32
2.2.1. PDB Selection and Molecular Modelling ……...… 32
2.2.2. Extraction of the Tetracyclic Pyridone Inhibitor from JAK2 Receptor .. 34
2.3. Conformational analysis …… 36
2.3.1. Generation of Methotrexate Conformers ……... 36
2.3.2. Extraction and Estimation of the Ligand Binding Energy and Ligand Binding Affinity of the Separate Methotrexate Conformers …….. 37
2.3.3. Determination of the Optimal Conformer ……..……. 38
2.4. Virtual Screening …….……. 38
2.4.1. Pharmacophore Generation for Virtual Screening …….……. 39
2.4.2. Screening of Hit Molecules ……...…. 43
2.4.3. Identification of Lipinski's Rule of Five Compliant Ligands ……..... 45
2.4.4. Protomol Generation and Molecular Docking ……...… 45
2.5. *De Novo* Design Approach ……...….… 46
2.5.1. Determining Protein-Ligand Interactions ……...… 47
2.5.2. Seed Structure Generation ……...…...… 47
2.5.3. Generation of *De Novo* Molecules ……..… 48
2.5.3.1. POCKET ……... 48
2.5.3.2. GROW ……...…… 49
2.5.3.3. PROCESS ……...….. 49
2.6. Molecular Analysis for Compliance to Lipinski's Rule of Five ……..….. 50
3. Results …….. 51
3.1. Conformational Analysis …….….… 52
3.1.1. Selection of the Best Conformer ……...…….....…. 52
3.2. Virtual Screening ……...……..... 54
3.2.1. Consensus Pharmacophore ……. 54
3.2.2. Filtration of Results ……..... 55
3.2.3. Ligands Generated through Virtual Screening ……...… 55
3.3. *De Novo* Growth ……... 57
3.3.1. Topology Mapping ……...….. 57
3.3.2. Ligand Binding Pocket Mapping …….. 58
3.3.3. Seed Generation ……...…….…… 60

3.3.4. Ligand Generated by Structure-Based Drug Design …….....…..... 61
3.3.5. Identification of the Highest Affinity *De Novo* Generated Molecules … 69
4. Discussion ……...……. 71
4.1. Rationale for the Study ……...……... 72
4.2. Analysis of Results of the Virtual Screening Approach …… ..……...….. 73
4.2.1. Analysis of ZINC00034158 ……... 75
4.2.2. Analysis of ZINC92898345 ……..... 76
4.2.3. Analysis of ZINC00002273 ……..... 77
4.2.4. Comparison of the Highest-Ranking Virtual Screening Molecule to the Optimal Methotrexate Conformer ……...……... 78
4.3. Analysis of Results of the *De Novo* Approach ……... 78
4.3.1. Analysis of the Highest Affinity *De Novo* Generated Molecule ……..… 79
4.3.2. Comparison of the Best Generated *De Novo* Molecule to the Optimal Methotrexate Conformer ……..... 81
4.4. Identification of the Amino Acids Critical to Binding ……..... 81
4.5. Comparison of *De Novo* and Virtual Screening …….....… 83
4.6. Conclusion ……...….....….. 84
4.7. Limitations …… 85

References ……...…….….. 86

List of Publications and Abstracts …….….. 93

Appendix I: Ethics Approval …….… 96

Addendum …….. 97

List of Tables

Table 1.1: The 2016 WHO diagnostic criteria for Polycythaemia Vera …...…….. 3

Table 1.2: JAK2 inhibitors and their ligand IDs …….…… 18

Table 2.1: Description of the different coloured regions in the pharmacophore …..….. 43

Table 2.2: Lipinski's Rule of Five ……..……. 45

Table 3.1: The number of analogous molecules generated in accordance to Lipinski's Rule of Five, before and after filtration on MONA® ……..…….…. 55

Table 3.2: The top 5 ligands obtained through Virtual Screening and their properties .. 56

Table 3.3: The seed structures generated during the *De Novo* method ……... 60

Table 3.4: *De Novo* ligands obtained from Seed 2 ……...……..…. 62

Table 3.5: *De Novo* ligands obtained from Seed 3 …….……. 66

Table 3.6: The top 3 molecules generated from Seed 2 and their properties …….…. 69

Table 3.7: The top 3 molecules generated from Seed 3 and their properties …...…..…. 70

List of Figures

Figure 1.1: The 2D structure of Hydroxyurea ……...……... 8

Figure 1.2: The 2D structure of Ruxolitinib ……...…….....… 10

Figure 1.3: The 3D structure of JAK2 bound to tetracyclic pyridone 6 by X-Ray diffraction with a resolution of 2.0Å ……...….… 15

Figure 1.4: The 2D structure of Methotrexate …….…… 19

Figure 2.1: The 3D structure of the Methotrexate molecule ……...… 33

Figure 2.2: The 3D structure of tetracyclic pyridone 6, extracted from PDB 2B7A ….. 34

Figure 2.3: The *apo* form of JAK2 ……...……...… 35

Figure 2.4: The 3D structure of the 20 different Methotrexate conformers …… 36

Figure 2.5: PDB 2B7A in 'Macromolecular View' …….....… 40

Figure 2.6: The tetracyclic pyridone inhibitor docked in PDB 2B7A, in 'Active View'.41

Figure 2.7: Pharmacophore of the tetracyclic pyridone inhibitor ……...…..... 41

Figure 2.8: Pharmacophore of the Methotrexate molecule ……...……..… 42

Figure 2.9: Pharmacophore of the Methotrexate molecule and tetracyclic pyridone-6 molecule superimposed ……...…... 42

Figure 2.10: The filters applied for hit molecule screening ……..... 44

Figure 2.11: The 8 databases searched for hit molecules ……...……. 44

Figure 2.12: The generated protomol …….. 46

Figure 3.1: The 3D structure of the optimal Methotrexate conformer ……... 53

Figure 3.2: Consensus pharmacophore representing the Methotrexate and Pyridone-6 scaffolds ……..……... 54

Figure 3.3: The 2D topology map indicating the critical interactions between the Methotrexate molecule and the amino acids lining the ligand binding pocket of JAK2 ……...……. 57

Figure 3.4: The pharmacophore for the optimal Methotrexate conformer generated using the POCKET module in LigBuilder® v1.2 ……..…. 58

Figure 3.5: The key site for the optimal Methotrexate conformer generated using the POCKET module in LigBuilder® v1.2 ……...…….…… 59

Figure 4.1: The 2D topology map indicating the ligand-receptor interactions between ZINC00034158 and the amino acids lining the ligand binding pocket of JAK2 ……75

Figure 4.2: The 2D topology map indicating the ligand-receptor interactions between ZINC92898345 and the amino acids lining the ligand binding pocket of JAK2 ….……76

Figure 4.3: The 2D topology map indicating the ligand-receptor interactions between ZINC00002273 and the amino acids lining the ligand binding pocket of JAK2 ……. 77

Figure 4.4: The 2D topology map indicating the ligand-receptor interactions between the highest affinity molecule of Seed 2 and the amino acids lining the ligand binding pocket of JAK2 ……..……. 80

List of Graphs

Graph 3.1: A graph of Ligand Binding Affinity (pKd) and Ligand Binding Energy ($kcalmol^{-1}$) against Methotrexate conformer number ……..…....……. 53

Graph 4.1: A graph of the common critical amino acids necessary for binding with the JAK2 ligand binding pocket vs frequency …….……... 82

List of Appendices

Appendix I: Ethics Approval ……...……...… 96

Glossary

2B7A	The PDB identification code for JAK2
Apo	A receptor in its unbound form
JAK2	A non-receptor tyrosine kinase that forms part of the Janus Kinase and Signal Transducer and Activator of Transcription pathway. It has an important role in cell growth, especially in controlling the production of blood cells from haematopoietic stem cells
Ligand Binding Affinity	The ability of a molecule to bind to an active site, via interactions with amino acids or hydrophobic areas lining the active site. It measures the strength of this bond and is measured in pKd
Ligand Binding Energy	The sum of the intermolecular interactions between the ligand and the target protein, measured in $kcalmol^{-1}$
Ligand Binding Pocket	A space within the target protein made up of amino acid residues, that possesses suitable properties for ligand binding
Pharmacophore	It describes the spatial arrangement of those features which are necessary for an interaction between a ligand binding pocket and a target molecule
Protomol	An idealised ligand binding pocket which defines the energetically unstable amino acids at the core of a protein
In silico	A method or prediction using a computational approach, either on a computer or via computer simulation, with respect to chemistry
Tetracyclic pyridone-6	A pan selective JAK2 inhibitor

List of Abbreviations

AL	Acute leukaemia
EPO	Erythropoietin
GH	Growth hormone
HBA	Hydrogen bond acceptor
HBD	Hydrogen bond donor
HCT	Hematocrit
HDAC	Histone deacetylase
HTC	Haematocrit
HU	Hydroxyurea
IFN-α	Interferon alpha
JAK	Janus Kinase
JH	JAK homology
LBA	Ligand binding affinity
LBE	Ligand binding energy
LBP	Ligand binding pocket
MPNs	Myeloproliferative Neoplasms
MTX	Methotrexate
NMR	Nuclear Magnetic Resonance
PDB	Protein data bank
PV	Polycythaemia Vera
Rux	Ruxolitinib
SAR	Structure-Activity Relationship
SPR	Structure-Property Relationship
STAT	Signal transducer and activator of transcription
TF	Transcription factor
VS	Virtual Screening
WHO	World Health Organization

Chapter 1

Introduction

1.1 Polycythaemia Vera

1.1.1 Brief Overview

According to the World Health Organization (WHO), myeloproliferative neoplasms (MPNs), more commonly known as blood cancers, can be further divided into 3 sub-groups – Polycythaemia Vera (PV), essential thrombocytosis and primary myelofibrosis (Spivak, 2017; Tefferi et al, 2018). In this study, we will be focusing mainly on PV, a disorder that occurs due to mutations in hematopoietic stem cells. These mutations cause certain mechanisms in the body, such as signal transduction pathways related to haematopoiesis, to become activated (Spivak, 2017).

PV, is a rare, hematologic disorder, marked by clonal proliferation of the progenitors found in the bone marrow. It then progresses to the abnormal production of erythroid cell line, which is not dependent on erythropoietin (EPO) (Finazzi & Barbui, 2007), with erythrocytosis being predominant. It is thus characterised by an increase in the production of inflammatory cytokines such as interleukin1-alpha from the malignant cells and from the stroma cells in bone marrow (Hasselbalch & Holmström, 2019). This clinical feature is characterised by an increase in red blood cell mass (Goerttler et al, 2005), in fact, this change is used as a diagnostic tool for PV (Barbui et al, 2011). The incidence of PV is quite rare, in fact, according to the latest studies, in the USA, it is estimated to be between 0.7 and 2.8 cases per 100 000 per year. The prevalence of PV is 44-57 cases per 100 000 persons yearly. Systemic symptoms that characterise this disease include fatigue, night sweats and also pruritus. Splenomegaly occurs in 36% of patients with PV. The association of PV with increased risk of thrombotic events and haemorrhagic events means that the chance for cardiovascular complications increases (Devos et al, 2017). Previous studies have been carried out in patients who were not yet receiving treatment.

The results showed a high occurrence of thrombotic events and the life expectancy was around one year and a half from the diagnosis (Finazzi & Barbui, 2007).

1.1.2 Diagnosis and Prognosis

PV is diagnosed by following the 2016 WHO diagnostic criteria, as can be seen in Table 1.1 below:

Table 1.1: The 2016 WHO diagnostic criteria for Polycythaemia Vera adapted from Devos et al, (2017)

Major criteria	I. Increase in haemoglobin level (>16.5g/dL in men and >16.0g/dL in women), increase in haematocrit level (>49% in men or >48% in women), or other evidence of increased red cell volume >25% above the normal count
	II. Bone marrow biopsy showing hypercellularity for age with trilineage growth
	III. *JAK2V617F* or JAK2 exon 12 mutations
Minor criteria	I. Serum EPO level below the normal reference range Endogenous erythroid colony formation in vitro

For diagnosis, there needs to be the recognition of either the 3 major criteria, or major criteria I and II, together with a minor criterion.

PV, is capable of gradually developing into another form of MPN, mainly myelofibrosis or acute leukaemia (AL). The progression of PV, is marked by the increased chances of the development of thrombotic complications, being the cause of an increasing in morbidity and mortality (Goerttler et al, 2005; Vannucchi, 2014). The life expectancy of a patient with PV is decreased to about 15 years after the diagnosis, when treated effectively (Goerttler et al, 2005). The chance of the occurrence of these clinical

manifestations is increased with age (>60 years), and in case of previous thrombotic events (Finazzi & Barbui, 2007).

The spontaneous conversion of PV into AL, has quite poor diagnosis. The incidence of this is about 7%, with chemotherapeutic treatment for PV increasing the chance of conversion into AL to 20% (Spivak, 2017). Until this moment, the aetiology of PV is still not known and it is quite a demanding task to differentiate between PV and secondary erythrocytosis. This puts scientists a step back when it comes to the development of rational drug design targeted therapy (Goerttler et al, 2005).

1.1.3 Gene Expression

The profiling of genes helps to discover the consequences that genetic abnormalities bring about when it comes to cellular processes occurring in the body. Patients suffering from MPNs have a different neutrophil gene expression from those that do not suffer from this disease. However, this neutrophil expression is the same for the 3 different subgroups of MPNs. In PV, there is the activation of genes that are associated with inflammatory signalling pathways, such as interleukin-6, interleukin-8, interleukin-10, transforming growth factor beta and also granulocyte-macrophage colony-stimulating factor (Spivak, 2017).

Furthermore, in PV, the haematopoietic stem cell gene expression differs further between men and women. The common factor between genders is the *JAK2V617F* gene (Spivak, 2017).

Gene expression profiling helps in the identification of mutations leading to PV and helps scientists in the generation of a molecular signature, which helps in diagnosing this rare disease. Studies show that patients with altered gene expression leading to the occurrence

of PV harbour anomalies in differentially expressed genes when compared to their healthy counterparts. Specifically, it was shown that up to 644 genes were differentially expressed in PV patients when these were compared to healthy subjects. Of these, 253 genes were up-regulated, whilst the remaining 391 were down-regulated. Further studies showed, that the transcription factor (TF) NF-E2, is involved in the cause of PV. This TF is expressed in the precursor haematopoietic cells and in those cells which are affected by PV. The abnormal expression of this TF can cause cells to differentiate into erythroid cells, leading to the maturation of these erythroid cells in the absence of EPO. Therefore, one can conclude that in PV patients, there is the overexpression of NF-E2 at the protein level by peripheral granulocytes (Goerttler et al, 2005).

The diagnosis process together with the risk assessment of the disease and the choice of drug therapy particular to it, is quite a complicated process (Spivak, 2017).

1.1.4 Haematopoietic Stem Cell Bone Marrow Niches

Haematopoietic stem cells can be found in “two specialized bone marrow niches” – the proliferative niche and the quiescent niche. The former is sinusoidal and it is the location where thrombopoietin promotes DNA synthesis. Moreover, macrophages here help to maintain erythroblasts. The quiescent niche on the other hand is endosteal and it is supplied with blood by the presence of arterioles and also innervated through sympathetic nerves. Here, stem cells are connected to both osteoblasts and thrombopoietin. The stem cells located in the quiescent niche are maintained by megakaryote secretions - CXCL4 and TGF-β1 (Spivak, 2017).

PV stem cells upregulate the inflammatory cytokine genes such as the CCL3 gene, tumor necrosis factor, LGALS3 and the LCN2 gene. Upon activation, these genes cause the

inhibition of normal stem cell proliferation. They also promote osteomyelofibrosis and damage the niche sympathetic nerves. This enhances the myeloproliferative process (Spivak, 2017).

1.1.5 Current Treatment

Currently, there is no cure for PV (Devos et al, 2017). The treatment being used targets more the associated risks that are characteristic to PV rather than PV itself, and it is individualized to the particular patient (Vannucchi, 2014). Myelosuppressive drugs are one of the regimen drugs used to reduce the rate of progression of thrombosis associated with PV. However, there is the risk that these drugs may in turn, increase the chance of the transformation of PV into AL. Due to these probabilities, the treatment for PV is adapted according to severity and progression of the disease. In fact, for low-risk patients, treatment is normally phlebotomy and low-dose aspirin.

Phlebotomy should be the main and first recommendation in PV patients, and it should be the only treatment in low-risk patients (McMullin et al, 2015). This intervention is performed twice a week at the start of the treatment, or on alternate days in cases where hematocrit (HCT) is more than 60%. Phlebotomy is continued until HCT levels become less than 45%. Blood counts are taken every 4-8 weeks so that phlebotomy frequency can be adjusted accordingly. Usually, younger patients are capable of allowing the removal of about 350 to 450 mL of blood. Smaller amounts of blood are withdrawn in elderly patients (Vannucchi, 2014).

Low-dose aspirin (100mg daily), when it is not contraindicated, is a drug which can also be given to all PV patients as prophylactic treatment for thrombosis. Coumarin derivates, low molecular weight (MW) heparin, rivaroxaban, apixaban, dabigatran or dipyridamole

are other prophylactic therapies which are sometimes used in low-risk PV patients. (Devos et al, 2017).

Higher risk patients are treated with cytotoxic therapy, including chemotherapy, with the drug of choice in this case being hydroxyurea (HU). Novel drugs, including alpha-interferon and imatinib, which have an effect on Janus Kinase (JAK) 2 expression, have not yet been used extensively in the management of PV, and are consequently used with caution in specific cases (McMullin et al, 2015).

Cytoreductive treatments, or treatments which result in the reduction of tumour cells, are used to treat the blood hyper viscosity that presents in PV. Cytoreduction is normally carried out through phlebotomy or chemotherapy. The target HCT level suggested by the 'Polycythaemia Vera Study Group', should be 0.45 for men and 0.42 for women. This finalised decision was taken from studies that showed that when HCT levels were greater than 45%, there was a significant correlation with thrombosis and cardiovascular complications. These values for target HCT have not yet been sufficiently validated and further research is required in this respect (Vannucchi, 2014; McMullin et al, 2015).

HU is the first line cytoreduction drug, administered in high-risk patients, but its leukemogenic characteristics should be well considered prior to initiation of treatment. The decision to use HU is sometimes made more complicated, owing to the fact that there are currently no studies available which document the risk of leukemogenic occurrences as a result of its administration. The fact that MPNs have the tendency of transformation even in the absence of any treatment, further complicates attempts at correlation with HU administration. Evidence also seems to indicate that administration of alkylating agents or radiophosphorus for PV management have increased chances of developing AL with the co-administration of HU. Again, however, the validity of these associations requires

further investigation since there is still not enough evidence to support the pharmacotherapeutic association to the transformation, or whether the transformation is just a normal part of disease progression (Finazzi & Barbui, 2007; Vannucchi, 2014).

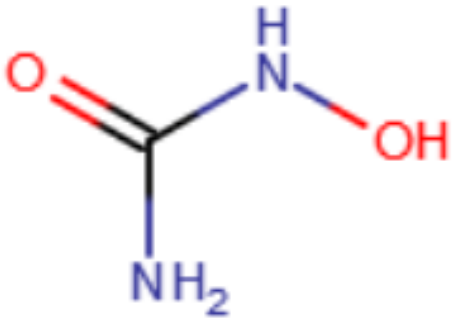

Figure 1.1: The 2D structure of Hydroxyurea rendered in Reaxys®[1]

Interferon alpha (IFN-α) is another drug used in PV, capable of inhibiting myeloproliferation and reducing the need for phlebotomy interventions. It suppresses the proliferation of the haematopoietic progenitors. It also inhibits the fibroblast progenitor cells located in the bone marrow and also stops the action of growth factor, transforming certain cytokines which are usually associated with the development of myelofibrosis. In a study carried out on 279 PV patients, 50% showed reduction in HCT on IFN-α treatment, 77% showed reduction in spleen size and 75% had reduction in pruritus (Finazzi & Barbui, 2007; Hasselbalch & Holmström, 2019). Significant improvement is

[1] RELX group. Reaxys® Structure Editor [Internet]. London: RELX group; 2019 [cited 2021 May 08]. Available from URL: https://www.reaxys.com/#/structure-editor

normally observed after 1-2 years of administration, to the extent that sometimes, a reduction in maintenance dose is possible, successfully keeping patients in remission. The use of IFN-α is limited due to expense, the fact that it requires parenteral administration and also due to its side effect profile. Most patients on IFN-α exhibit flu-like symptoms and fever. Chronic use causes weakness, myalgia, depression and cardiovascular symptoms. This may lead to discontinuation of use of this drug when the adverse effect profile starts to outweigh the benefits of treatment (Finazzi & Barbui, 2007).

The limitations associated with the treatment options for PV discussed thus far explains why there is significant treatment failure risk associated with PV. Often, currently available treatments do not significantly improve the burden that comes with PV, and sometimes, patients can no longer tolerate drug treatment, or develop resistance to it. Resistance is most commonly associated with HU administration. Furthermore, it has been shown that resistance to HU is associated with a greater risk of transformation. The corollary therefore is that there is much scope for the development of a treatment that prevents disease progression and transformation. No such treatment is currently available to improve these unmet needs (Devos et al, 2017).

The most recent drug used for the management of PV is Ruxolitinib (rux). This drug is a JAK inhibitor and has yielded promising results in PV management, maintaining steady HCT levels without phlebotomy requirement, and being well tolerated by patients. The experience with rux has been considered as promising, to the extent that JAK2 is being considered as an important target in PV management, and with research into the development of JAK2 inhibitors being considered as the way forward for PV management (Geyer & Mesa, 2014; McMullin et al, 2015).

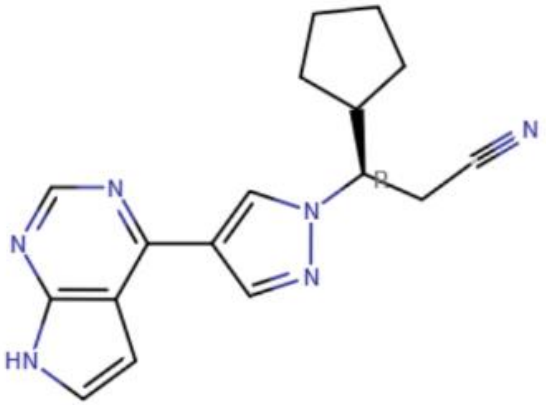

Figure 1.2: The 2D structure of Ruxolitinib rendered in Reaxys®[1]

Apart from the essential pharmacological treatment, lifestyle changes are also recommended, to aid in the reduction of cardiovascular complications. Emphasis is made on the importance of quitting smoking in smokers, control of body weight, introducing physical exercise on a daily basis, adhering to medications for hypertension, diabetes, and cholesterol if applicable, avoiding the use of oral contraceptives which have a tendency of increasing the risk of thrombosis, and avoiding situations that increase the chances of bleeding (Vannucchi, 2014).

[1] RELX group. Reaxys® Structure Editor [Internet]. London: RELX group; 2019 [cited 2021 May 08]. Available from URL: https://www.reaxys.com/#/structure-editor

1.2 JAK2

1.2.1 Overview

A mutation which was discovered in 2005 in the *JAK2V617F* gene, located in the 1849th site of this same gene, was found to lead to the development of PV (Barbui et al, 2011; Zhang et al, 2017). More than 90% of patients affected with PV have this mutation, making them biologically distinct (Barbui et al, 2011). In fact, according to Tefferi et al, (2018), the distribution frequency of this driver mutation is approximately 99%. This mutation most commonly occurs on exon 14, however, in some patients, this mutation might occur over exons 12, 13 and 14 (Tefferi et al, 2018). This new finding has changed the way and improved the criteria looked into when diagnosing, monitoring and assessing the response of treatment for MPNs (Barbui et al, 2011). Various studies have been conducted, and information has been collected in this regard. The pathways through which *JAK2V617F* causes myeloproliferation have been studied and are well documented (Grinfeld & Godfrey, 2017).

This mutation is known to affect JAK2 function by weakening the effect of the JAK homology 2 (JH2) structure domain of JAK2 on inhibiting autophosphorylation. This means that there is an increase in phosphorylation of JAK2 (Zhang et al, 2017).

In a study which was carried out, MPN patients who hadn't yet started treatment were grouped into a mutation positive group and a mutation negative group. When signalling molecules p-JAK2, p-STAT3 and p-STAT5, which are protein molecules associated with the JAK2 Signal Transducer and Activator of Transcription (STAT) pathway, were compared between the patients of these two subject groups, the mutation positive group had a significantly higher protein expression than the mutation negative group. The same study also suggested that in the presence of this mutation in MPNs, there is an increase

in the expression of a number of cell proliferation genes, which is in fact a characteristic of MPNs. Moreover, this mutation will activate both the intrinsic and extrinsic coagulation pathway, thus increasing the risk of thrombosis associated with MPNs (Zhang et al, 2017).

Even though this activation of JAK2 has brought about an increase in the interest of the development of JAK specific small molecule inhibitors, there still hasn't been any change in the way MPNs are managed (Barbui et al, 2011).

Such pathways include the activation of the JAK/STAT signalling, however, this myeloproliferation could also take place through other canonical or non-canonical pathways. A number of mechanisms show how this specific mutation can be linked with well-defined clinical diseases, showing how constitutional and attained or acquired factors can interact in the presence of a single mutation to bring about a specific disease phenotype (Grinfeld & Godfrey, 2017). Since each individual JAK forming part of the JAK family has its own specific and particular roles when it comes to oncogenesis and the pathology of the immune system, the need for specific inhibitors for the specific members of this family has been realised, where targeting specifically the conserved ATP-binding sites seems to be one of the approaches being considered (Williams et al, 2009). Although a significant amount of information is available regarding this receptor, some questions remain unanswered about its association with PV, specifically regarding how the *JAK2V617F* affects the function of stem cells and what mechanisms cause myelofibrotic and leukemic transformation. Current treatment options focus mainly on cardiovascular event prevention. Targeting the JAK2 mutant clone, in order to be able to reverse underlying marrow pathology and therefore avoid the development and transformation of PV, represents a very attractive way forward (Grinfeld & Godfrey, 2017).

1.2.2 Mode of Action

Literature shows that JAK2 represents a viable target for mitigation of the progression of PV. JAK2 is found on chromosome 9 and the p24 band (He et al, 2016). It forms part of the non-receptor JAK family, which has a role in growth, proliferation, and in the differentiation of numerous cells. It is activated through ligand binding (Kurzer et al, 2004). The JAK/STAT signalling pathways are required for cell proliferation and differentiation, but also apoptosis.

The most important downstream target for JAK is found to be the STAT family. The STAT family is composed of 7 classes – STAT1 to STAT4, STAT5A, STAT5B, STAT6 (Nicolas et al, 2012). The process of activation mainly involves JAK2 phosphorylation when it binds to a ligand, which then cause the downstream phosphorylation of STAT3 and STAT5. The phosphorylated STAT3 and STAT5 can then form dimers, which in turn enter within the nucleus and start the expression of a number of genes (Zhang et al, 2017). Specifically, when a ligand binds to receptors of this family, such as the growth hormone (GH) receptors, cytokine receptors and leptin receptors, dimerization occurs. Following this the JAK molecule binds to these receptors, and when two JAK macromolecules are proximal, there is prompt trans-phosphorylation, causing their activation and in turn the activation of downstream targets (Nicolas et al, 2012). This phosphorylation process normally occurs in HepG2 cells (Siveen et al, 2014).

Another mode of activation for JAK is through G-protein coupled receptors, protein tyrosine kinases and also through a change in the intracellular calcium (Nicolas et al, 2012).

The JAK/STAT pathway takes on an important role in promoting cell survival, growth, differentiation and inflammatory processes. It has been discovered that this pathway is

also involved in the leptin-induced neuroprotection, and in the control of food intake. Alzheimer's disease is also associated to the JAK/STAT pathway. Even though the mechanism that this pathway uses when involved in neuronal function is still not known, studies showed that JAK is capable of regulating the gene expression of certain neurotransmitter receptors and their function. Such receptors include the GABA receptor and the muscarinic acetylcholine receptor (Nicolas et al, 2012).

Due to its mode of action, and the signalling pathways that JAK forms part of, its activity is related to a number of haematopoietic diseases and malignancies including PV, some cardiovascular diseases and also certain immune-related disorders (Williams et al, 2009).

1.2.3 JAK2 Ligand Binding Pocket

A study carried out to determine the crystalline structure of JAK2 was done using a 2.0Å resolution and in complex with pyridone-6, also known as 2-tert-butyl-9-fluoro-3,6-dihydro-7Hbenz[h]-imidaz[4,5-f]isoquinoline-7-one, which readily binds to JAK2, inhibiting it (Lucet et al, 2005).

This is described in PDB 2B7A (Lucet et al, 2005), the same receptor used in this study, as seen in Figure 1.3:

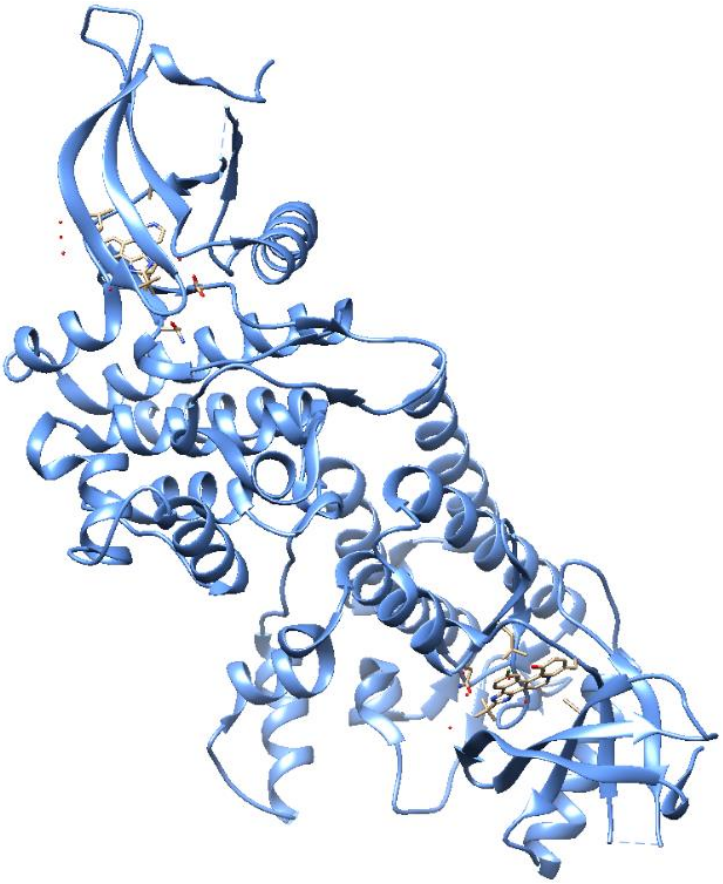

Figure 1.3: The 3D structure of JAK2 bound to tetracyclic pyridone-6 by X-Ray diffraction with a resolution of 2.0Å rendered in UCSF Chimera® v.1.12 (Petterson et al, 2004) based on the PDB 2B7A (Lucet et al, 2005)

As mentioned previously, JAK2 dimerizes, with the root mean square deviation between the two molecules being 0.56Å. The study focused mainly on one monomer (Lucet et al, 2005).

All members of the JAK family posses an identical domain structure, having a C-terminal protein tyrosine kinase domain, JH1, next to a kinase like-domain known as JH2, together with five other JAK homology domains (JH3-JH7) (Lucet et al, 2005).

The basic structure of JAK2 consists mainly of a compact N-terminal composed of 5 anti-parallel β sheets and an α helix, and a substantial C-terminal lobe, consisting of 8 α helices and 3 of 3/10 helices, and 6 anti-parallel β strands, which are paired up (Lucet et al, 2005).

What makes the JAK2 enzyme different from the other kinases is that it has a loop structure known as the insertion loop between amino acid 1056 and amino acid 1078. It is not tightly fitted next to the C-terminal base, making it quite movable especially in solvents. The exposed serine which is located at position 1056, and which can be found in all JAK tyrosine kinases, is thought to be essential in the phosphorylation dependent regulatory role that these receptors have. The activation loop for JAK2 is made up of residues 994 to 1023, in which there is a phosphorylation site. The phosphorylation of Tyr^{1007} is shown to be essential for its activity. When activated, Tyr^{1007} and Tyr^{1008} are phosphorylated, and a salt bridge is formed in between Lys^{882} and Glu^{898}. Stabilization of this active state of the molecule is achieved through various interactions. Such interactions include those between 2 antiparallel β sheets, β9/β6 and β10/β11, and 2 arginine residues. There are also interactions between Arg^{971}, which binds to the base of the activation loop, whilst Arg^{975} interacts to its base. Lys^{1005}, Lys^{1009}, and Lys^{1030} stabilize $pTyr^{1007}$. $pTyr^{1008}$ is stabilized by Lys^{999}. $pTyr^{1007}$ is located near the outer part of the molecule, exposing it to solvents, thereby making it important in the degree of substrate binding. When compared to the structure of other kinases, the JAK2 tyrosine kinase has a more closed opening angle, due to the N-terminal lobe being closer to the C-terminal lobe. This “constriction” is increased further because of the conformation of the glycine loop and activation loop mentioned previously. This conformation presents a ligand binding pocket (LBP) for JAK substrates (Lucet et al, 2005).

1.2.4 Endogenous Agonism of JAK2

Cytokines are the main activators of JAK. The mechanisms with which they do so is still not confirmed, but it is known that there are about 30 class I and 12 class II cytokine receptors which are related to the activation of JAK. The JAKs bind to the mentioned receptors through their N-terminal 4.1, through Ezrin, Radixin and Moesin domain, and they bind to the receptors conserved membrane which is rich in proline. GH receptor, is a class I cytokine receptor which activates JAK2.

1.2.5 JAK2 Inhibitors

A number of potential molecules which have JAK inhibition properties have undergone testing for their possible indication in MPNs, however, only a few have been successful, primarily because of toxicity issues (Verstovsek & Bose, 2017). In fact, Molecule AZD1480, crystallised in protein data bank (PDB) deposition 2XA4 (Ioannidis et al, 2011), an orally active inhibitor for both JAK1 and JAK2, which leads to the inhibition of STAT, was undergoing clinical trials (Siveen et al, 2014), however it was discontinued due to neurological events development associated with its use. Molecule XL109 clinical trial was also discontinued due to the same events (Verstovsek et al, 2017).

To date, JAK2 inhibitors position themselves in the ATP binding site where there is an adenine base, located between the N and the C terminal lobes. This binding site is highly conserved, making it more specific (Lucet et al, 2005).

Table 1.2: JAK2 inhibitors and their ligand IDs adapted from Alexander et al, (2019)

Ligand	Ligand ID	Number of Lipinski's rules broken
Ruxolitinib	5688	0
AZD1480	5933	0
JAK inhibitor I/ Pyridone-6	5992	0
Baricitinib	7792	0
Pacritinib	7793	0
AT-9283	7949	0
Itacitinib	8364	0
Fedratinib	5716	1

An important aspect that should be kept in mind when designing or repurposing drugs for use in MPNs is that another mechanism of action that occurs in these diseases is the downregulation of JAK2 via the action of histone deacetylase (HDAC) inhibitors on HSP90 chaperone molecule through a process of acetylation. In fact, synergism between both JAK2 inhibitors and HDAC inhibitors has been proven in MPNs. When rux was administered in combination with drug molecule NCT01433445, an HDAC inhibitor, during a clinical trial, there was a decline of more than 20% in the *JAK2V617F* allele burden in 5 patients by week 48 (Verstovsek & Bose, 2017).

1.3 Methotrexate

1.3.1 Overview

Literature indicates that Methotrexate (MTX), a folate reductase inhibitor, (Strober & Menon, 2005; Fiehn, 2011) is also capable of JAK2 inhibition (Chinnaiya et al, 2017). MTX is known to inhibit the enzyme dihydrofolate reductase, therefore it blocks and prevents the synthesis of thymidylate and then purines and pyrimidines (Fan et al, 2012).

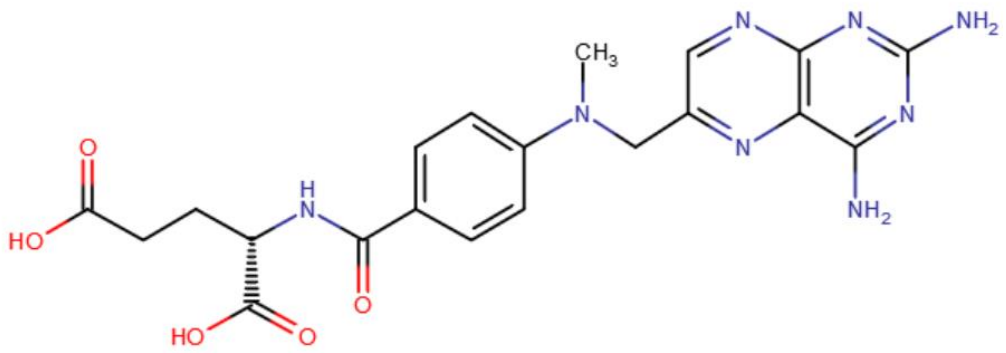

Figure 1.4: The 2D structure of Methotrexate rendered in Reaxys®[1]

The study concerning MTX and the effect that it has on JAK2 inhibition started from rux, a JAK1/2 inhibitor described in section 1.1.5, which showed benefits in survival for PV patients. Even though rux is effective, there is still limited availability and access to it due to it being expensive (Wade et al, 2013). Moreover, in the long term, it was seen that its efficacy is reduced. Its side effects, including increased infection rates, and a decrease in haemoglobin and platelet levels also need to be monitored closely and can be quite serious

[1] RELX group. Reaxys® Structure Editor [Internet]. London: RELX group; 2019 [cited 2021 May 09]. Available from URL: https://www.reaxys.com/#/structure-editor

(Passamonti & Maffioli, 2018). Due to this, JAK/STAT pathway inhibition was further investigated to discover more affordable and accessible drugs with a better side effect profile.

MTX, a cheap generic, was found to be a potential candidate (Chinnaiya et al, 2017). This molecule, being a dose-dependent STAT phosphorylation inhibitor, (Chinnaiya et al, 2017) does not, however, affect other phosphorylation dependent pathways (Thomas et al, 2015). Indications for this drug include arthritis, psoriasis and its use as a chemotherapeutic agent, meaning that its use treats both inflammatory and immune disorders, both controlled by the JAK/STAT pathway (Weinblatt, 2013). These effects support the hypothesis that the use of low-dose MTX could have the same effect on MPNs, including PV (Chinnaiya et al, 2017).

Clinical studies were conducted to analyse how MTX affects the JAK2 enzyme. One study was carried out on mice, where their JAK2 locus was swapped for the human JAK2 V617F allele, leading to PV symptoms when homozygous. The mice were treated with either low-dose MTX or a low-dose of vehicle control for 28 days. Diseased homozygous hJAK2 V617F mice normally have spleens with higher levels of pSTAT5 and pSTAT3 and increased mRNA levels of the JAK2/STAT5 target gene PIM1. Both *in vitro* and *in vivo* results demonstrated that the administration of MTX resulted in reduced levels of both pSTAT5 and pSTAT3, and also lead to lower levels of the pathway target gene PIM1. This therefore confirmed the *in vitro* test results and proved that *in vivo*, MTX is capable of inhibiting the JAK/STAT pathway (Chinnaiya et al, 2017).

Successive studies for the positive control regarding the hJAK2 V617F-expressing mice were carried out. These were administered either MTX or rux. Both heterozygous and homozygous mice had reductions in haemoglobin levels, red blood cell counts and HCT

levels. Even though MTX was found to have similar effects to rux, its treatment did not seem to cause myelosuppression in wild type mice. Both the controls and MTX treated mice still gained weight. Treatment with MTX adjusts white cell count to normal levels, however white blood cell subtypes are not affected (Chinnaiya et al, 2017).

Splenomegaly, was reduced with MTX treatment. Homozygote mice have "erythroid hyperplasia with red pulp expansion and loss of normal architecture, with occasional megakaryote clusters". These were alleviated with MTX since it decreases erythroid infiltration, with better formation of white pulp. Some wild type mice still had spleen enlargement, related to hypersplenism and red cell demolition. Reticulocyte count was increased. Here, MTX was not causing myelosuppression, unlike with rux, owing to the fact that the bone marrow is still capable of erythropoiesis, and reticulocyte response. In these wild type mice, there was a small incrementation in pSTAT5 and PIM1 mRNA levels after MTX treatment. More studies are required in order to try and explain the reasons for these observations, which might be related to MTX-induced lymphoma (Chinnaiya et al, 2017).

An *in silico* study was also conducted, using a high resolution form of the JAK2 JH1 kinase domain as a potential target to dock both MTX and ATP. MTX is thought to displace ATP since it has a higher affinity to the ATP ligand binding site of the kinase, acting as a type 1 kinase inhibitor (Chinnaiya et al, 2017).

The results obtained suggest that MTX, at low doses, inhibits the JAK/STAT signalling pathway, and also decreases splenomegaly and haematologic phenotypes related to the hJAK2 V617F-based mice model of human MPNs. To further confirm the results, a case study indicated that two MPN patients being administered low-dose MTX, had haematologic improvements (Chinnaiya et al, 2017).

Even though tests were carried out in mice, clinical trials should be opted for, to ensure the safe and effective use of MTX in this indication (Chinnaiya et al, 2017).

The way in which MTX inhibits the JAK/STAT pathway is still unknown. MTX is usually administered with folinic acid to alleviate any side effects (Strober & Menon, 2005). From data which was collected, it was confirmed that this drug combination had no effect on MTX's action, probably because both drugs enter the cells using the same transporter. One way in which MTX works might be that it lowers the pathological overactivation of JAK/STAT pathway to an extent where it is capable of controlling the disease without stopping the receptors physiological activation that is required for haematopoiesis or responses to infections. Also, since STAT5 phosphorylation in $CD34^+$ cells in MPN patients is only 1.5 fold greater than in healthy patients, mild suppression lasting for some time can be enough to control the disease (Thomas et al, 2015).

A more recent study was conducted on PV positive patients who were taking MTX for indications other than PV. Although the data is not conclusive, it suggested that in combination with other cytoreductive treatment, MTX might increase their effectiveness. Moreover, when used alone, it has a tendency of causing a reduction in platelet count as well as the frequency and the severity of symptoms associated with PV, especially those related to inflammation due to its potential suppression of pro-inflammatory cytokines (Francis et al, 2019).

1.3.2 Traditional uses of Methotrexate

MTX is a drug which is known to be administered in cancer patients as a chemotherapeutic drug for more than 40 years, due to its immune system suppression properties. However, recently, new indications have been discovered, including its usage

as a standard drug in patients suffering from rheumatoid arthritis, as an anti-rheumatic drug, and in other areas such as dermatology in patients suffering from psoriasis, mycosis fungoides, dermatomyositis and pityriasis rubra pilaris. The latter three indications for MTX still do not have FDA approval. It is also sometimes indicated in pneumology. Less common indications include pregnancy termination, in ectopic pregnancy and also in Crohn's disease. MTX is still not licensed by the FDA for use in severe Crohn's disease. Patients usually tolerate MTX, consequently decreasing problems of non-compliance. Any side effects which might occur during the treatment with MTX are reversible upon withdrawal (Weinstein GD, 1977; Joint Formulary Committee, 2016).

MTX is a once weekly drug which is normally administered in conjunction with folic acid on different days, since the latter prevents the occurrence of certain adverse effects that this drug brings about. Moreover, this drug should be avoided in pregnancy as studies have shown that it has teratogenic characteristics (Joint Formulary Committee, 2016).

1.4 Drug Repurposing

1.4.1 Overview

The drug repurposing process aims to make use of drugs that are already available on the market for a particular indication (March-Vila et al, 2017). Throughout the repurposing process, various chemical and structural changes are done to the concerned, readily available drug molecule, via different software available online. These changes allow for the molecule to fit into its newly discovered target receptor (Pantziarka et al, 2014).

1.4.2 Advantages of Drug Repurposing

Unlike in the case of newly discovered and developed drugs, which require significant research to synthesize, in drug repurposing, the drug is an already well-known pharmaceutical agent which has been used for some time and already has its use within the community. This gives us a lot of information about the drug itself, its structure, and the way that it works, through a plethora of data which is available to researchers. Such data typically includes information regarding the pharmacokinetics of the drug, any adverse effects, its bioavailability and metabolism by the body (Pantziarka et al, 2014).

Phase I trials of repurposed drugs are at times avoided, since enough data is available to warrant elimination of this step. The money which is saved from this can be dedicated to other sections of the research program. However, this is not the case in all repurposed drugs as sometimes, Phase I trials can still be a requirement so that maximum tolerated doses can be determined, since dosage regimens vary from one indication to another. Also, drug combinations might be part of the newly discovered dosage regimen and therefore toxicity and drug-drug interactions would require further studies (Pantziarka et al, 2014).

The use of already existing drugs for new indications provides with a short-circuit of the original process used in newly discovered drugs, and this is in fact proven in one review concerning the comparison of drug repurposing to *de novo* drug development. It takes from 10 – 17 years for *de novo* development, whilst the process of repurposing a particular drug takes from 3 – 12 years (Pantziarka et al, 2014).

Apart from the economic benefit that drug repurposing has, risk reduction is also a great benefit for industrial pharmaceutical companies. The number of potential drugs for a particular condition, and then the actual amount of drugs that ultimately make it to the

market is very low, and therefore the repurposing method is opted for with the aim that through reusing existing drugs of known pharmacological properties, failure would be reduced (Pantziarka et al, 2014).

The usage of low cost and generic drugs is another advantage to repurposing. Pharmaceutical companies need to make profit and therefore they first require to make up for the expenditure for the research and development of the drug, and then they require income to be able to invest in new studies. The long developmental process and research associated with the development of new drugs, together with the various tests and clinical trials that are required, lead to an increase in the cost of the drugs that are then placed on the markets. These are not always affordable to patients who require them to be able to lead an acceptable life. This also puts a lot of stress on health systems in the country and it could sometimes be unaffordable for the country to provide the concerned patients with the free medication. On the other hand, repurposed drugs are available as either generics or at a low cost. This is an important factor for the countries healthcare system. Moreover, patients tend to go for medications that are cost efficient for them, and therefore these low cost, generic repurposed drugs would probably be bought more than the costly new drugs (Pantziarka et al, 2014).

Lastly, patients who are good candidates for the repurposed drug could be put in the clinical trial. This not only provides researchers with the essential human participants required for the study, but it also has a positive impact on the patients who would be administered the tested drug which has known toxicity data, and can therefore be managed (Pantziarka et al, 2014).

1.4.3 Disadvantages of Drug Repurposing

The debate of property rights of the drug and patents poses a disadvantage for pharmaceutical companies, and it is therefore sometimes quite a risky move in deciding to repurpose a drug which belongs to other companies. Also, certain drugs might show potential good characteristics for the treatment of a particular disease only to find out through clinical trials that a therapeutic effect is achieved at a dose which is far in excess of the maximum tolerated dose. This poses a high risk of the occurrence of side effects and toxicity, which would decrease the efficacy and thereby popularity of the drug (Pantziarka et al, 2014).

1.5 *In silico* Techniques

1.5.1 Computational Drug Design

The rational drug design process takes on a multidisciplinary approach. Drug design is a process which enables scientists in the discovery of relatively new medicines. It is based on the already known knowledge regarding biological targets (Mandal et al, 2009).

During the drug design process, specialized programs are used, with the intention of creating molecules that work in one of three ways:

- Molecules that inhibit the function of other molecules by binding competitively and with higher affinity than the molecule that would normally bind to a particular receptor.
- By inhibiting the existing interactions between the molecule and its ligand.
- By activating endogenous molecules that are not working efficiently due to a diseased state of the patient.

Contemporary drug design techniques have improved drastically through the introduction of new and improved technologies including 3D-ray and Nuclear Magnetic Resonance (NMR) structures of the molecules, and the creation of docking tools (Mandal et al, 2009).

The rational drug design process can be subdivided in two parts. The first and most common approach is through the design of molecules having ideal properties for their binding with already well-known targets whose 3D structure and any other relevant information is known. The second approach is the design of small molecules to bind with targets whose structural details regarding its LBP can be known or unknown. The information on the latter can be obtained by analysing gene expression in samples where one group is treated with the drug and another group is untreated (Mandal et al, 2009).

The choice of lead molecules depends on various factors including:

- Molecule's affinity and specificity to the LBP
- Hydrophilicity and lipophilicity of the drug
- ADME
- Electrophilicity and nucleophilicity
- Toxicity
- Structure- Activity Relationship (SAR)
- Structure- Property Relationship (SPR)

The use of software facilitates the process, rendering it one with more accurate predictions and filtering molecules to come up with the ones that have the best potential in proceeding to further steps in the drug design process (Mandal et al, 2009). In fact, molecular docking, due to it being a fast and ideal method to screen large molecular and target libraries, has been in use to predict the ability of a specific drug to bind to a specific target.

This is possible by predicting the geometry of the target as well as the interactions of a complex with a particular small molecule ligand (March-Vila et al, 2017).

1.5.2 Software

Some software used during this project include:

- UCSF Chimera® v.1.12 (Petterson et al, 2004)
- SYBYL®-X 1.1 (Ash et al, 2010)
- ZincPharmer® (Koes & Camacho, 2012)
- BIOVIA® Discovery Studio 2020[2]
- LigandScout® (Wolber & Langer, 2005)

UCSF Chimera® v.1.12

UCSF Chimera® v.1.12 (Petterson et al, 2004) envisions the molecular structure and related data regarding the molecules. It presents high quality images which are useful in identifying conformational constitutes.

ZincPharmer®

ZincPharmer® (Koes & Camacho, 2012) is a program found online which allows for the research of the Zinc database, which can be bought. This program offers a special tool for

[2] Dassault Systèmes. BIOVIA Discovery Studio Visualizer. Version 20.1 [Software]. San Diego: Dassault Systèmes; 2020 [cited 2021 Jul 26]. Available from URL: https://www.3dsbiovia.com/products/collaborative-science/biovia-discovery-studio/visualization-download.php

the design and improvement of molecules through refining of molecular structures. One can also search for conformers.

BIOVIA® Discovery Studio 2020[2]

With BIOVIA® Discovery Studio 2020 one can investigate hypothesis *in silico* before attempting any experiments. This program allows for the visualization of molecules and the binding with their respective receptor. The interactions between the two are then shown in 2D and 3D images. Ligand binding energy can also be determined.

LigandScout®

LigandScout® (Wolber & Langer, 2005) is a program used for the generation of pharmacophores, either from a structural point of view or from a ligand-based view. From a structural point of view, the program uses macro molecule ligand complexes. On the other hand, from a ligand-based view, the program compares the ligands and determines the similarities between them.

[2] Dassault Systèmes. BIOVIA Discovery Studio Visualizer. Version 20.1 [Software]. San Diego: Dassault Systèmes; 2020 [cited 2021 Jul 26]. Available from URL: https://www.3dsbiovia.com/products/collaborative-science/biovia-discovery-studio/visualization-download.php

1.6 Aims

This literature review has highlighted a number of important issues. It has evidenced that PV is a rare disease that nonetheless comes with its significant risk of mortality. It has also highlighted the fact that current treatments produce limited success, and that more research into this disease state is necessary if its high risk of mortality is to be reduced (Devos et al, 2017). The fact that PV is a rare disease implies that often, there is lack of funding for research, with innovator pharmaceutical companies preferring to divert funds into conditions with higher prevalence (Pantziarka et al, 2014). The fact that there is evidence in the literature that MTX is capable of JAK2 inhibition, and that this has a mitigating effect on PV progression (Chinnaiya et al, 2017), represents a significant advantage owing to the fact that MTX is an old molecule about which there is a wealth of synthetic clinical, pharmacological, pharmacokinetic and toxicity data. The fact that MTX and its analogs could be repurposed as JAK2 inhibitors is attractive, from the point of view of the cost-cutting that drug repurposing inherently implies, which is even more significant in the context of rare diseases where funding is typically scarce (Pantziarka et al, 2014).

There is consequently evidence emanating from the literature that this is a valid area of research (Chinnaiya et al., 2017). Specifically, this study aims to use the MTX scaffold, to model the critical interactions between it, and JAK2. Based on this data, MTX analogs will be identified and designed. The optimal structures will be validated and proposed for molecular dynamics simulation studies.

Chapter 2

Methodology

2.1 Introduction

In this *in silico* study, the main focus was the JAK2 receptor and the way with which the MTX molecule binds to it at specific points within its LBP. Therefore, this study aimed to probe the JAK2 LBP, and identify, through both a virtual screening (VS) approach, and a *de novo* approach, analogs, that are capable of targeting JAK2 in a similar way to MTX. A ligand-based drug design approach was taken to choose the best conformer for JAK2, where the ligand having the highest ligand binding affinity (LBA), and the lowest ligand binding energy (LBE), was chosen as the optimal conformer.

2.2 Protein Data Bank Depositions

2.2.1 PDB Selection and Molecular Modelling

Crystallographic deposition PDB 2B7A (Lucet et al, 2006), describes the bound co-ordinates of JAK2 in complex with a pan-JAK inhibitor, having the ideal resolution of 2.0 Å. Resolution is an important aspect in the determination of a crystal structure of a molecule, since it helps in defining that molecule's atomic orientation. This makes it easier for one to choose the appropriate and ideal conformers. The ideal resolution would be between approximately 1.5 Å and 3Å, since this is the resolution at which most proteins are capable of diffracting, leading to a more resolved model (Smyth & Martin, 2000).

The inhibitor binds to JAK2 via what is known as an induced fit mechanism. The mentioned inhibitor is tetracyclic pyridone-6, specifically 2-*tert*-butyl-9-fluoro-3,6-dihydro-7*H*-benz[h]-imidaz[4,5-*f*]isoquinoline-7-1. Interactions with specific residues

that are known to be specific to the JAK family were seen between the receptor and the tetracyclic pyridone itself (Lucet et al, 2006).

PDB 2B7A (Lucet et al, 2006), which can be seen in Figure 1.3 was downloaded from the online repository RCSB PDB (Berman et al, 2000) which can be found available online on the URL http://www.rcsb.org/.

The MTX molecule that was used as a ligand for JAK2 was sketched and modelled on SYBYL®-X 1.1 (Ash et al, 2010).

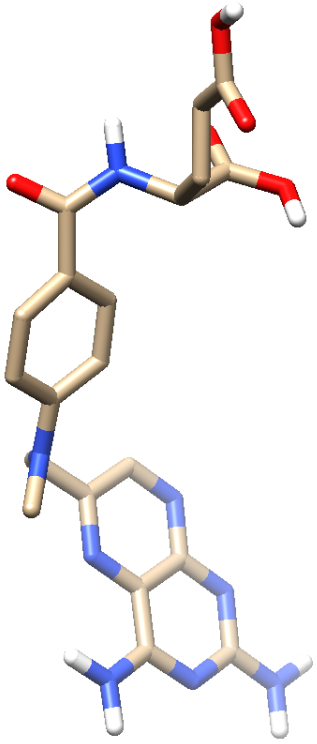

Figure 2.1: The 3D structure of the Methotrexate molecule sketched in SYBYL®-X 1.1 (Ash et al, 2010) and visualized in UCSF Chimera® v.1.12 (Petterson et al, 2004)

2.2.2 Extraction of the Tetracyclic Pyridone Inhibitor from JAK2 Receptor

Modelling of the *apo* form of the JAK2 receptor was carried out in SYBYL®-X 1.1 (Ash et al, 2010). PDB crystallographic deposition 2B7A (Lucet et al, 2006) was retrieved to obtain the crystallographic complex of JAK2 bound to the tetracyclic pyridone ligand. This inhibitor was then extracted. Molecules which were regarded as not important for ligand binding, such as water molecules, were removed. This was done with the aim of improving computational speed. The extracted ligand was saved as a separate MOL2 file, whilst the *apo* JAK2 receptor was saved in PDB format for future use. The LBE for tetracyclic pyridone-6 was also calculated using SYBYL®-X 1.1 (Ash et al, 2010). This was then later used as a reference to be able to choose the best MTX conformer for JAK2.

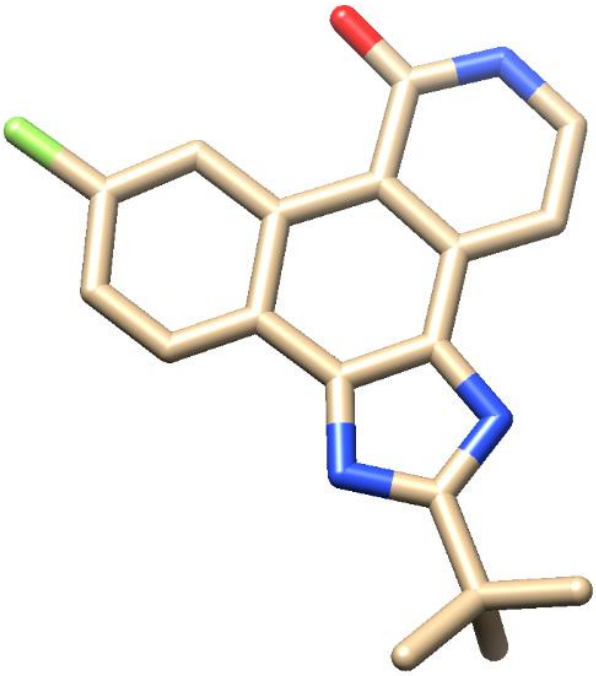

Figure 2.2: The 3D structure of tetracyclic pyridone-6, extracted from PDB 2B7A (Lucet et al, 2006) rendered in UCSF Chimera® v.1.12 (Petterson et al, 2004)

The *apo*JAK receptor was then exported and saved as a PDB file without a bound ligand. This PDB file was later on necessary for conformational analysis carried out using X-Score® v1.3 (Wang et al,2002).

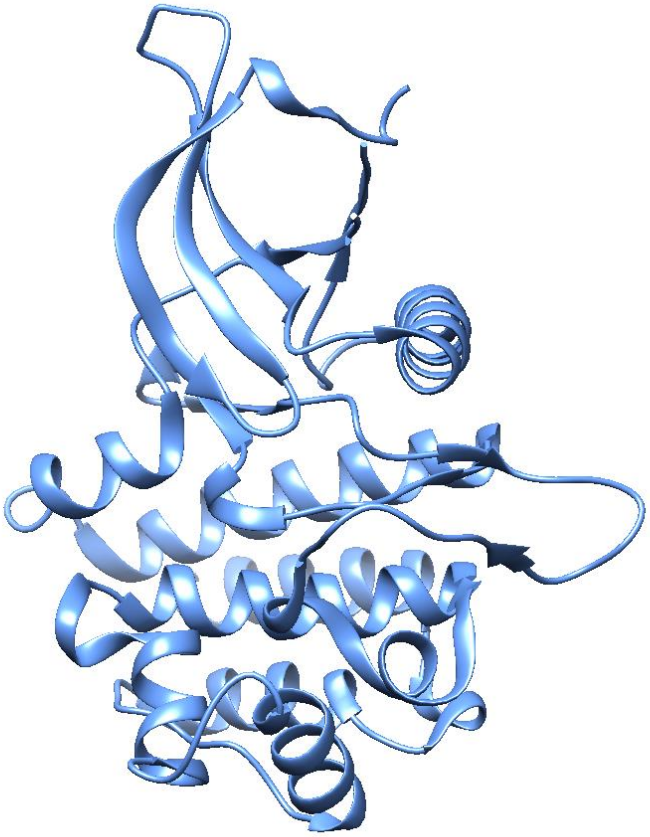

Figure 2.3: The *apo* form of JAK2 rendered in UCSF Chimera® v.1.12 (Petterson et al, 2004), based on PDB 2B7A (Lucet et al, 2006)

2.3 Conformational Analysis

2.3.1 Generation of Methotrexate Conformers

The main aim of this study, as previously mentioned, was to identify the optimal conformation of the MTX molecule within the JAK2 LBP, using 2B7A (Lucet et al, 2006) as the template molecule. Using the 'Similarity Suite' algorithm on SYBYL®-X 1.1 (Ash et al, 2010), a number of MTX conformers for 2B7A (Lucet et al, 2006) were generated. This step ensured that there was the maximal use of the JAK2 LBP, as the conformational space within the JAK2 LBP was identified as well as the optimally binding MTX conformers. The previously sketched MTX molecule was docked into the *apo*JAK receptor and conformational analysis was carried out so as to identify the optimal binding position of the MTX molecule. The lead molecule was allowed motion within the receptor to allow for the generation of the different position with which the MTX molecule could sit in the LBP. This process generated 20 conformers.

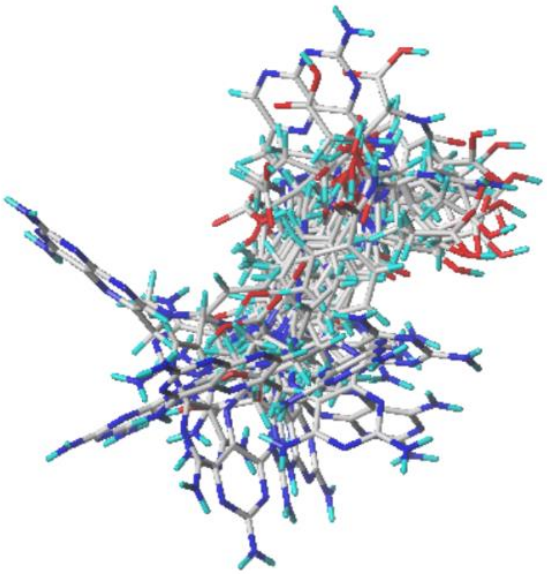

Figure 2.4: The 3D structure of the 20 different Methotrexate conformers rendered in SYBYL®-X 1.1 (Ash et al, 2010)

2.3.2 Extraction and Estimation of the Ligand Binding Energy and Ligand Binding Affinity of the Separate Methotrexate Conformers

Every conformer, with its different positioning in the ligand binding region, was selected, exported and saved as a separate file in a process known as extraction. This was done for each of the 20 conformers. Due to the fact that the MTX molecule had different spatial arrangements, the conformers were grouped according to their positioning within the LBP.

The energy of each individual conformation of MTX was measured in SYBYL®-X 1.1 (Ash et al, 2010). Every conformer, one by one, was imported onto SYBYL®-X 1.1 (Ash et al, 2010), and its energy was computed in $Kcalmol^{-1}$. The necessary data containing LBE was recorded onto a separate Microsoft Word document. It is important to note that the conformers with a lower LBE were the ones that were preferred since ideal molecules do not require a high amount of energy to separate them from the receptor.

X-Score® v1.3 (Wang et al, 2002) was then used for calculation of the LBA of the different conformations of MTX within the JAK2 LBP. The PDB file containing the *apo* form of JAK2 and the MOL2 files of the MTX molecules were imported and X-Score® v1.3 (Wang et al,2002) was run. The MOL2 files were inputted separately for each conformer, and X-Score® v1.3 (Wang et al, 2002) was run every time. The affinities for all the MTX conformers were recorded and saved as separate PDF files. The *apo* form of JAK2 was also run with the JAK inhibitor of 2B7A (Lucet et al, 2006), to calculate its affinity so that it could then be used as a baseline molecule with which comparison could be made. In this case, those molecules having a higher affinity were preferred over low affinity conformers since molecules that bind tightly to the LBP are preferred.

2.3.3 Determination of the Optimal Conformer

To determine which of the MTX molecules had the best orientation within the JAK2 LBP, a linear graph of LBE and LBA vs MTX conformer number was plotted. The values obtained previously for the LBE as well as the LBA were copied into a Microsoft Excel sheet and a graph was automatically plotted. This consisted of a linear line graph, with the LBE in $Kcalmol^{-1}$ on the left y-axis, the LBA (pKd) on the right y-axis, and MTX conformer number on the x-axis. The graph was analysed and examined further to determine which MTX molecule could be considered as being the most optimal. The optimal conformer was selected on the basis of maximum peak height difference between LBE ($Kcalmol^{-1}$) and LBA (pKd). Therefore, the best MTX conformer was chosen on the basis of having a low LBE but a high LBA.

2.4 Virtual Screening

A ligand-based VS approach was used in this study. Such an approach has been in use for quite some time in the drug discovery industry. The main aim for using VS was that a library of small molecules were docked into a specific LBP and from these, we identified which of the molecules are preferably chosen to be moved forward for testing for when it was required to choose the hit molecules. Through this process, we were capable of differentiating between those molecules which were active and those which were inactive. In doing so, the number of molecules being considered as possible hits was reduced, making the drug design discovery approach simpler and much cheaper, especially when compared to high throughput screening (Kontoyianni, 2017).

2.4.1 Pharmacophore Generation for Virtual Screening

Interactions that molecules form with their respective target molecules can be represented through a 3D arrangement of abstract features which represent interactions such as hydrogen bonds, hydrophobic and aromatic interactions and so on, rather than functional groups (Kaserer et al., 2015). The pharmacophore describes the spatial arrangement of the necessary interactions of the target molecule with the bioactive ligand (Koes & Camacho, 2012).

In this study, the pharmacophore was generated using the software LigandScout® (Wolber & Langer, 2005), which allowed the use of a specific tool to create a pharmacophore built on the topology of the binding site of the receptor in question (Kaserer et al, 2015).

PDB 2B7A (Lucet et al, 2006), was loaded onto LigandScout® (Wolber & Langer, 2005), and 3D pharmacophores were produced. The interactions between the receptor-ligand complex were analysed. A macromolecular view of JAK2 was loaded and the co-ordinates of the ligands bound to it were generated. As can be seen in Figure 2.5, PDB 2B7A (Lucet et al, 2006) shows a dimer complex.

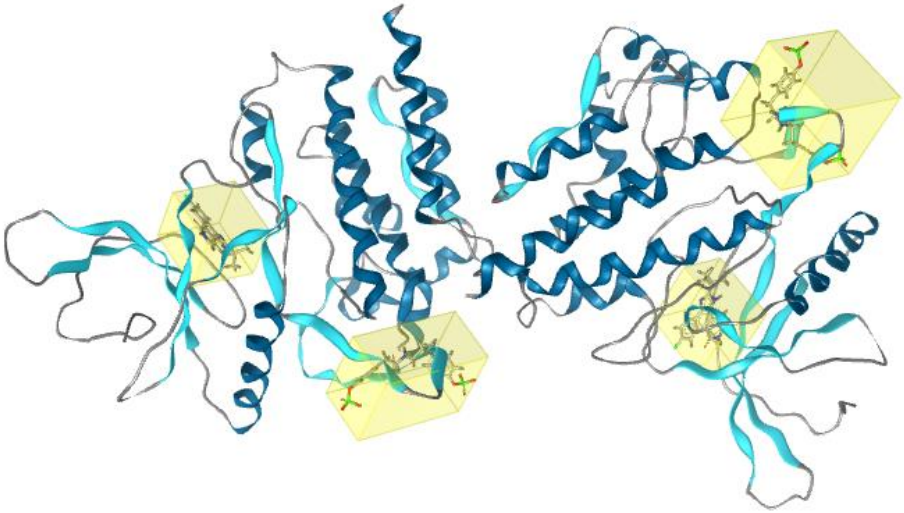

Figure 2.5: PDB 2B7A (Lucet et al, 2006), in 'Macromolecular View' rendered in LigandScout® (Wolber & Langer, 2005)

Using the 'Active View' tool in LigandScout® (Wolber & Langer, 2005), the interactions between the amino acid chain of the JAK2 LBP, and the tetracyclic pyridone inhibitor were further evaluated.

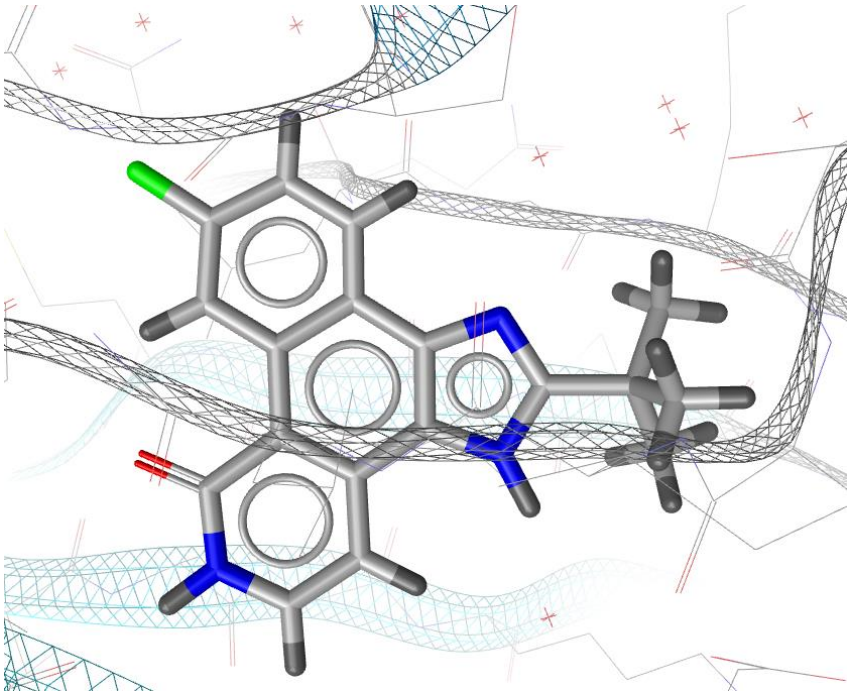

Figure 2.6: The tetracyclic pyridone inhibitor docked in PDB 2B7A (Lucet et al, 2006), in 'Active View' rendered in LigandScout® (Wolber & Langer, 2005)

The pharmacophore for the tetracyclic pyridone was generated using the 'Create Pharmacophore' algorithm.

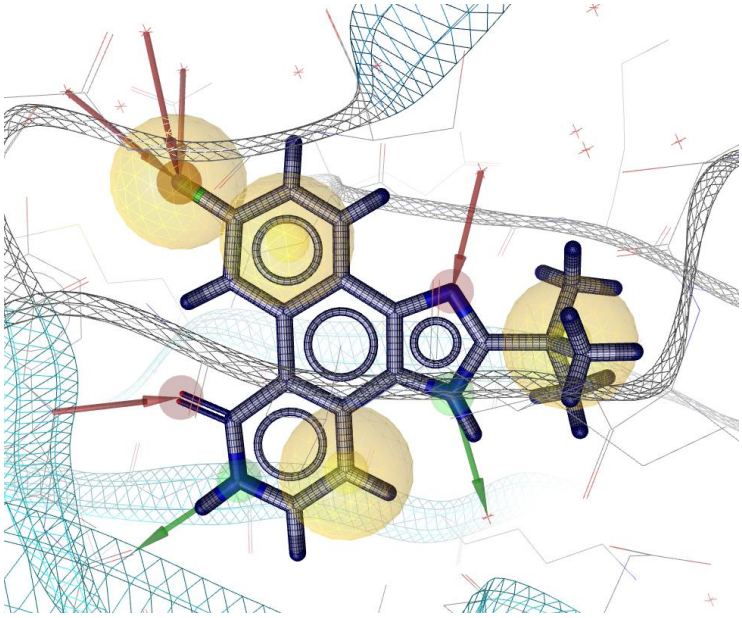

Figure 2.7: Pharmacophore of the tetracyclic pyridone inhibitor docked in PDB 2B7A (Lucet et al, 2006), rendered in LigandScout® (Wolber & Langer, 2005)

The same process was done for the optimal MTX molecule, to produce its pharmacophore;

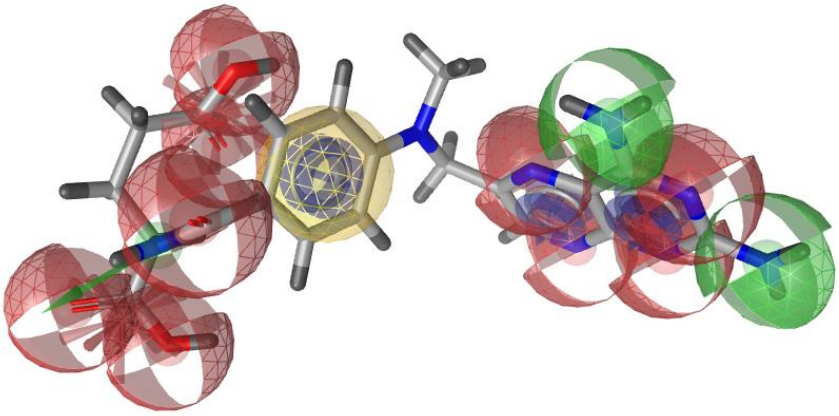

Figure 2.8: Pharmacophore of the Methotrexate molecule, rendered in LigandScout® (Wolber & Langer, 2005)

The tetracyclic pyridone molecule and the MTX molecule were superimposed onto one another to generate a pharmacophore of the two superimposed molecules.

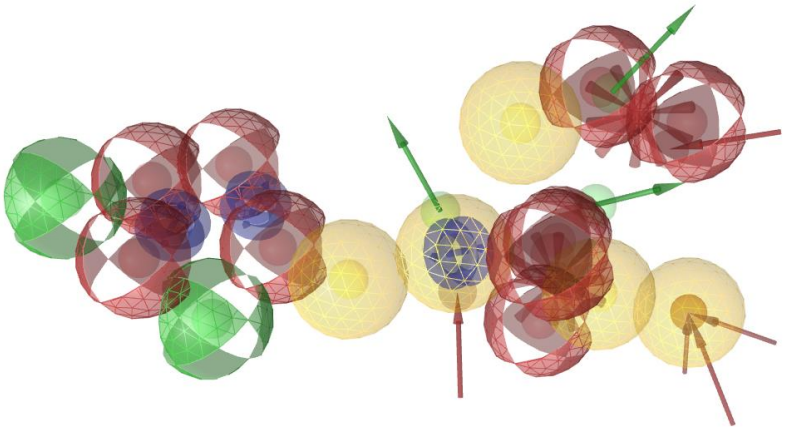

Figure 2.9: Pharmacophore of the Methotrexate molecule and tetracyclic pyridone 6 molecule superimposed, rendered in LigandScout® (Wolber & Langer, 2005)

The two pharmacophores were then superimposed and an average pharmacophore including all the critical contact points forged by the two molecules was generated. This step yielded a more robust query structure.

The following table summarizes what the different coloured regions and arrows refer to in the Figures above:

Table 2.1: Description of the different coloured regions in the pharmacophore

Colour	Refers to
Red arrow	Acceptor atom
Green arrow	Donor atom
Yellow spherical region	Hydrophobic area
Red spherical region	Acceptor region
Green spherical region	Donor region
Star shaped structure	Negative ionisable region

2.4.2 Screening of Hit Molecules

Screening for hit molecules involved the use of the online search engine ZincPharmer® (Koes & Camacho, 2012). This database contains a large chemical library of purchasable molecules. When a specific pharmacophore is loaded onto it, the database starts to search for molecules in these libraries which could match that specific pharmacophore (Koes & Camacho, 2012).

The consensus pharmacophore generated as stated in section 2.4.1 above was loaded onto ZincPharmer® (Koes & Camacho, 2012). Filters were applied to ensure that the hits identified had a lead-like nature. The number of maximum total hits was limited to 300 molecules so as to minimize having a larger number than necessary of molecules.

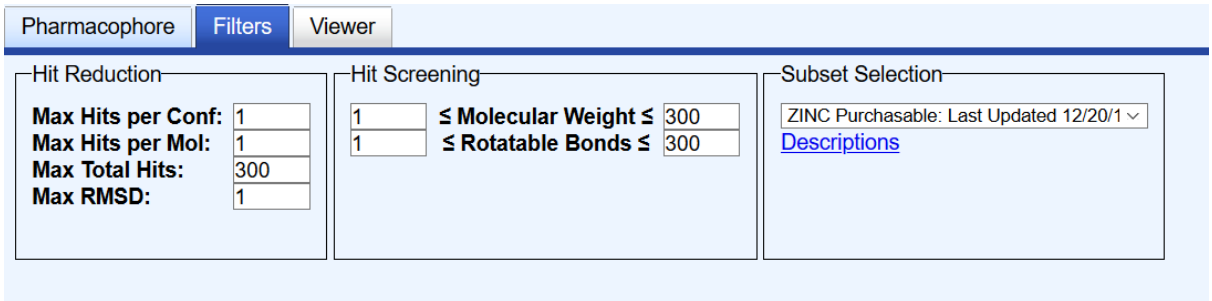

Figure 2.10: The filters applied for hit molecule screening rendered in ZincPharmer® (Koes & Camacho, 2012)

8 databases were searched to find lead-like hit molecules. For every database, the 'submit query' tool was used and all the hits found were saved collectively for each of the 8 different databases.

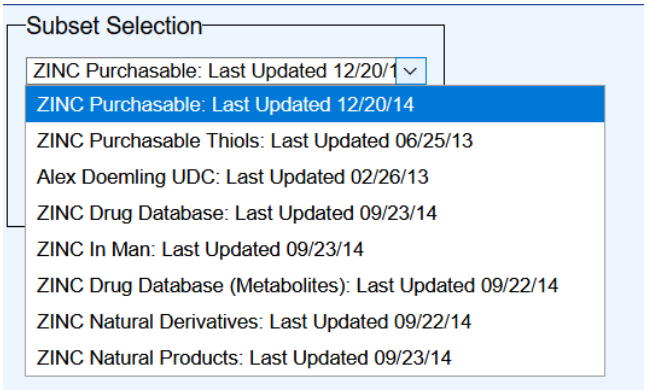

Figure 2.11: The 8 databases searched for hit molecules, rendered in ZincPharmer® (Koes & Camacho, 2012)

2.4.3 Identification of Lipinski's Rule of Five Compliant Ligands

The hit molecules previously generated on ZincPharmer® (Koes & Camacho, 2012) were then imported onto the desktop application MONA® (Hilbig & Rarey, 2015). The latter is a simple to use application which does not require expertise. The development of such an application was mainly due to the fact that since a large number of chemical molecule libraries have become increasingly available online, tasks like browsing of molecules, analysis and filtering of such molecules has become very common (Hilbig & Rarey, 2015).

The hit molecules were filtered in accordance to Lipinski's Rules. This Rule of five states that those molecules having the following criteria are more likely to have better absorption and permeation, making them more orally available (Lipinski et al, 2001):

Table 2.2: Lipinski's Rule of Five adapted from Lipinski et al, (2001)

MW	≤ 500
LogP	≤ 5
Hydrogen bond donors	≤ 5
Hydrogen bond acceptors	≤ 10

2.4.4 Protomol Generation and Molecular Docking

A protomol was generated with the intent of simulating the required and ideal interactions between the ligand and the amino acid chains of the LBP, thus making it an ideal docking site (Jain, 2009).

The protomol, representing energetically unstable amino acids which could be found at the interior core of JAK2, was modelled in SYBYL®-X 1.1 (Ash et al, 2010). The 'Surflex

Simulation' tool was used to do so. This process ranked all the previously obtained hits according to their affinity for the JAK2 LBP, leading to the identification of the best hit molecule.

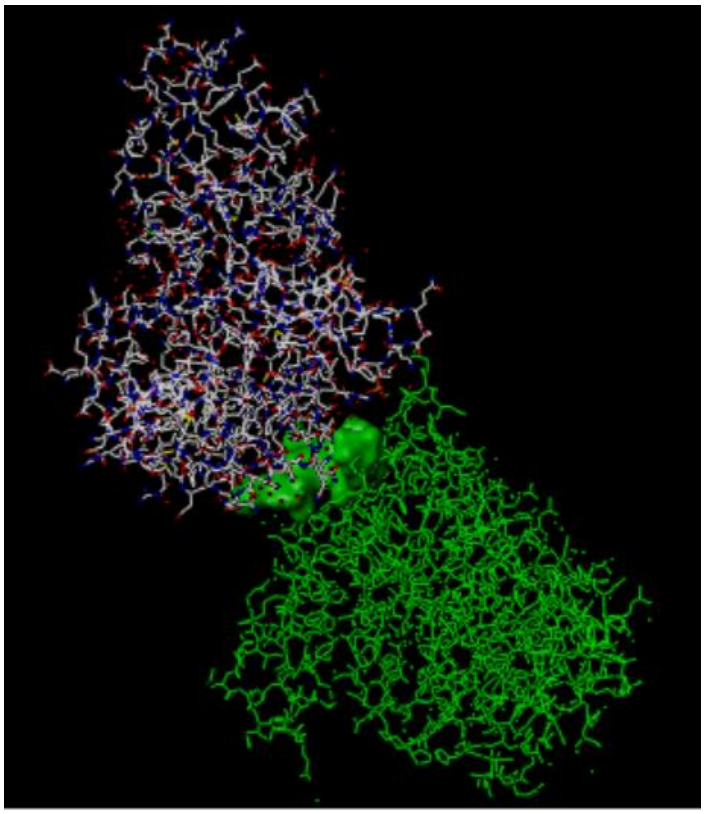

Figure 2.12: The generated protomol rendered in SYBYL®-X 1.1 (Ash et al, 2010)

2.5 *De Novo* Design Approach

In this part of the study, the identification of all the moieties present on the ligands, which are responsible for forging critical interactions with the LBP, therefore eliciting a biological response, was a crucial step. A 2D topology map, highlighting the interactions between the JAK2 LBP and the optimal MTX conformer was generated. This aided in the identification of fundamental atoms necessary for this interaction to occur.

2.5.1 Determining Protein-Ligand Interactions

The interactions forged between the receptor and the ligand were visualized using BIOVIA Discovery Studio®[2] . PDB 2B7A (Lucet et al, 2005) representing the JAK2 receptor, and the optimal MTX ligand were uploaded onto the software, and a topology map, depicting a number of interactions which were necessary for biological activity, was generated.

2.5.2 Seed Structure Generation

The generation of the topology map was an important step which aided in the creation of ideal seeds through a fragmentation exercise which generated a number of small molecules. It allowed for decision making when it came down to choosing which moieties on the optimal MTX molecule to retain, eliminate, modify or allow for additional growth. Seed structures were modelled in SYBYL®-X 1.1 (Ash et al, 2010). All the crucial moieties associated with necessary interactions with the receptor and ligand stabilisation within the binding pocket were retained during seed structure modelling. The moieties which could be seen to contribute to instability during the binding process, or which were irrelevant to binding, were computationally removed, and replaced with anchorage sites capable of sustaining novel growth. These anchorage sites were designated as special hydrogen atoms (H.spc).

[2] Dassault Systèmes. BIOVIA Discovery Studio Visualizer. Version 20.1 [Software]. San Diego: Dassault Systèmes; 2020 [cited 2021 Jul 26]. Available from URL: https://www.3dsbiovia.com/products/collaborative-science/biovia-discovery-studio/visualization-download.php

2.5.3 Generation of *De Novo* Molecules

De novo growth was carried out using LigBuilder® v1.2 (Wang et al, 2000), which is a multi-purpose program that allowed for a number of computational operations such as linking and growing to allow for the manipulation of molecular structures.

LigBuilder® v1.2 (Wang et al, 2000) is comprised of 4 modules: POCKET, GROW, LINK and PROCESS. The POCKET module analyses the LBP and identifies the important moieties within the LBP necessary for binding. It also prepares all the data necessary to be used by the GROW and LINK modules. These are the algorithms through which *de novo* molecular growth is sustained. The difference between the two algorithms is that while pre-designated anchorage point, the LINK algorithm tethers two fragments into a single entity using two anchorage points - one on each fragment.

2.5.3.1 POCKET

The POCKET module was used to build a 3D LBP map that highlighted the key interaction sites which a hypothetical ligand for a given LBP could occupy. It also recommended the best pharmacophore established on the key interactions. In fact, prior to the creation of the *de novo* molecules, analysis of the JAK2 receptor and its LBP was carried out. Potential binding sites were assessed, taking note of both the chemical and geometric information. This helped in outlining the binding site for the molecules as well as getting a clearer idea of the parameters of the LBP.

In this study, the PDB version of the *apo* JAK2 receptor was looked into, and the bioactive conformation of the MTX ligand, saved in .mol2 format, was used as a probe in order to elucidate the JAK2 LBP and to generate a pharmacophoric structure for ligands of this LBP.

The PDB file for the *apo* JAK2 receptor and the .mol2 file format for the best MTX conformer and the .mol2 file format of the seed were used to generate the 3D map of the JAK2 receptor.

2.5.3.2 GROW

The LBP map of the JAK2 receptor modelled in the POCKET module of LigBuilder® v1.2 (Wang et al, 2000) was taken to represent the pharmacophoric space within which *de novo* molecular growth could be sustained. The modelled seed structures were consequently docked into the JAK2 LBP map. The seed structures as designed could only sustain unidirectional growth. For this reason, *de novo* growth was carried out using the GROW module of LigBuilder® v1.2 (Wang et al, 2000).

2.5.3.3 PROCESS

The next step included applying the PROCESS algorithm of LigBuilder® v1.2 (Wang et al, 2000). For each molecular cohort that was generated for every seed structure, a molecular database that contained molecules that were segregated according to pharmacophoric similarity and ranked according to their LBA (pKd) was created.

For those seeds which were successful, a set of *de novo* molecules were generated and collected into a file. Another file contained information for all the *de novo* molecules generated during the process for each successful seed. Information contained within this file included the family number, MW, logP, binding score and chemical score.

This data was transferred onto a Microsoft Excel sheet and the molecules were filtered according to Lipinski's Rule of Five (Lipinski et al, 2001).

2.6 Molecular Analysis for Compliance to Lipinski's Rule of Five

The *de novo* molecules identified in the PROCESS module of LigBuilder® v1.2 (Wang et al, 2000) were filtered for Lipinski Rule (Lipinski et al, 2001) compliance. Only these latter molecules were retained for final analysis.

A structural analysis was carried out between the different families and their molecules. This was an important step in the identification of structural features that are essential for the interaction between the LBP and the corresponding molecule.

Chapter 3

Results

3.1 Conformational Analysis

The way with which a molecule binds to a receptor, greatly affects its LBA (pKd) and LBE (kcalmol^{-1}). Because of this, MTX was processed through SYBYL®-X 1.1 (Ash et al, 2010) to generate a number of conformers. In this way, the optimal conformer that bonded to the JAK2 LBP in the best conformational fit was chosen. 20 different binding poses were generated. Each conformer was numbered for identification in later stages. The choice of the optimal MTX conformer ensured that this molecule had the best bioactivity within the JAK2 LBP. Conformers' LBA (pKd) ranged between 4.64 and 5.81 whilst LBE (kcalmol^{-1}) ranged from 80.800 to 103.408.

3.1.1 Selection of the Best Conformer

The data obtained *in silico* was plotted on a line graph in order to obtain a better visualisation of the best conformer. The molecule having the highest LBA (pKd) and the lowest LBE (kcalmol^{-1}) was chosen as the optimal MTX conformer. The LBE (kcalmol^{-1}), which was calculated on SYBYL®-X 1.1 (Ash et al, 2010) and the LBA (pKd), which was calculated on X-Score® v1.3 (Wang et al,2002) can be seen on the y-axis of Graph 3.1 below. Each of the 20 conformers are represented on the x-axis of Graph 3.1 below. The baseline affinity of the tetracyclic pyridone to JAK2 was calculated and used as a reference. MTX conformer 09 was chosen as the optimal conformer.

Graph 3.1: A graph of Ligand Binding Affinity (pKd) and Ligand Binding Energy (kcalmol^{-1}) against Methotrexate conformer number

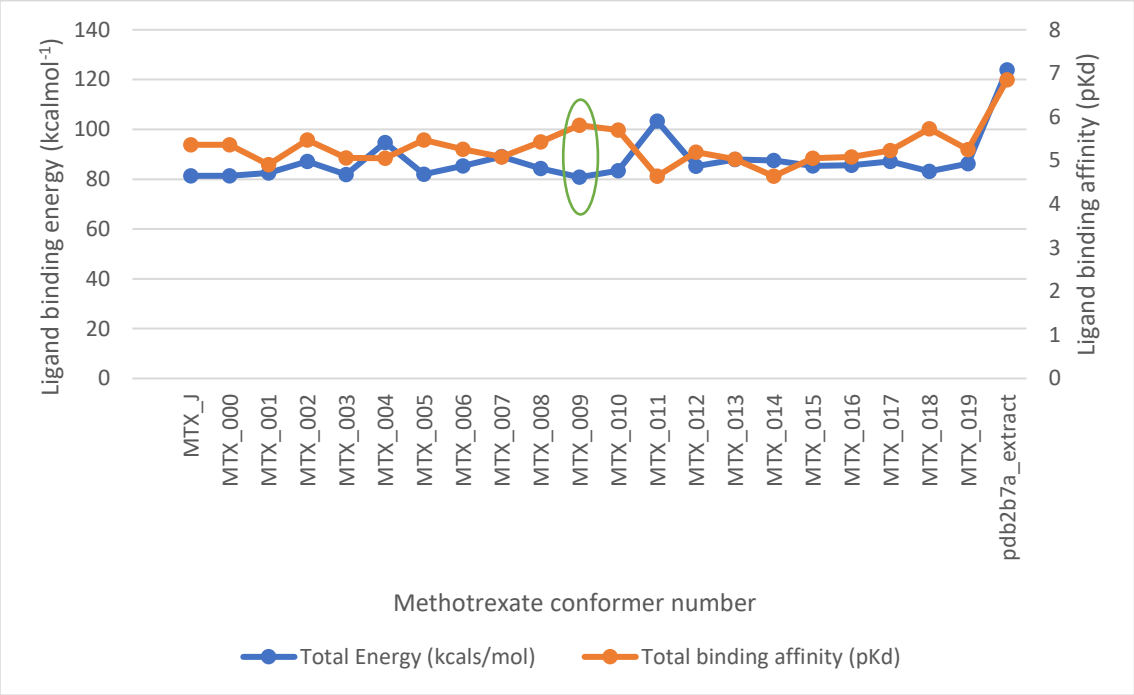

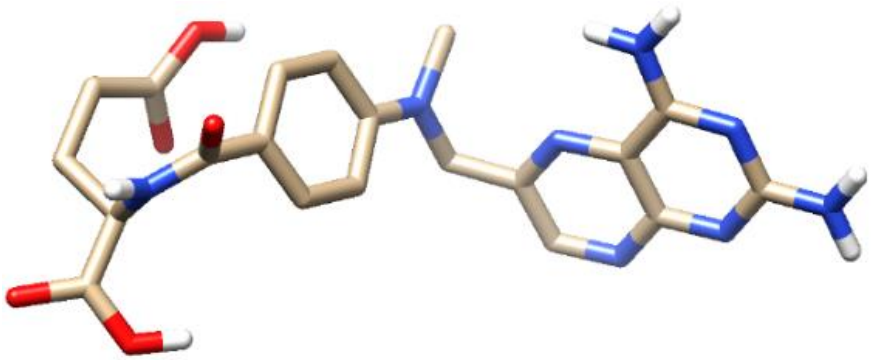

Figure 3.1: The 3D structure of the optimal Methotrexate conformer, rendered in UCSF Chimera® v.1.12 (Petterson et al., 2004)

3.2 Virtual Screening

3.2.1 Consensus Pharmacophore

When the pharmacophore for tetracyclic pyridone-6, and the pharmacophore for MTX were superimposed, they produced a consensus pharmacophore which combined the structure activity requirements of both molecules, as can be seen in Figure 3.2. The red spherical region represents an acceptor region whilst the yellow spherical region is a representation of a hydrophobic area.

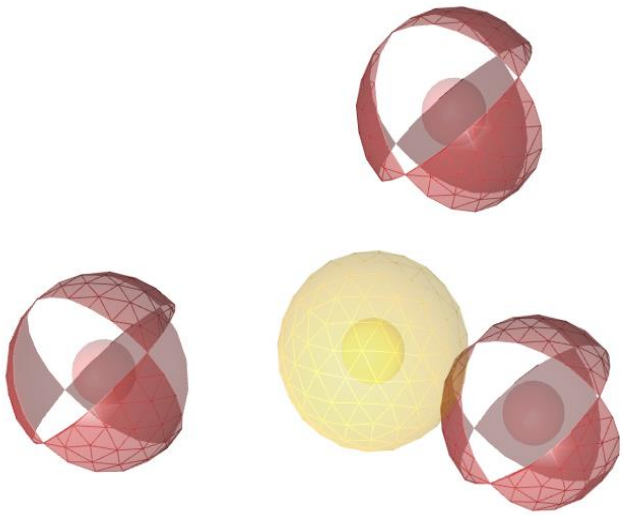

Figure 3.2: Consensus pharmacophore representing the Methotrexate and Pyridone 6 scaffolds modelled in LigandScout® (Wolber & Langer, 2005)

3.2.2 Filtration of Results

The desktop application MONA® (Hilbig & Rarey, 2015) was used to filter the generated molecules in accordance to Lipinski's rules (Lipinski et al, 2001).

Table 3.1: The number of analogous molecules generated in accordance to Lipinski's Rule of Five (Lipinski et al, 2001), before and after filtration on Mona® (Hilbig & Rarey, 2015)

Database	Analogous molecules generated	Analogous molecules after filtration
Alex Doemling UDC	14	12
ZINC Purchasable	292	161
ZINC Purchasable Thiols	289	176
ZINC Drug Database	113	31
ZINC in Man	256	104
ZINC Drug Database (Metabolites)	279	85
ZINC Natural Derivatives	272	157
ZINC Natural Products	275	127

3.2.3 Ligands Generated through Virtual Screening

The Lipinski Rule compliant ligands were docked computationally within the protomol and then were ranked according to their physicochemical properties in addition to their affinity for the JAK2 LBP.

Table 3.2: The top 5 ligands obtained through Virtual Screening and their properties. 3D images were rendered in UCSF Chimera® v.1.12 (Petterson et al., 2004). 2D images were rendered in MONA® (Hilbig & Rarey, 2015)

3D Structure of Hit Molecule	2D Structure of Hit Molecule	Total Score
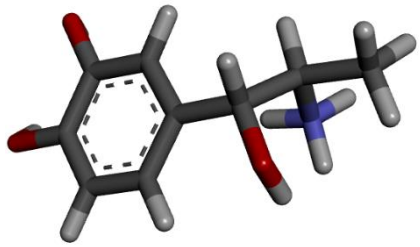 ZINC00034158	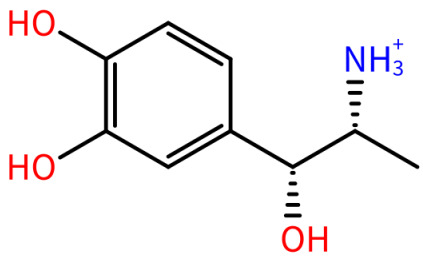	6.03
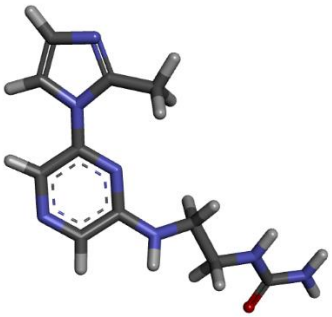 ZINC92898345	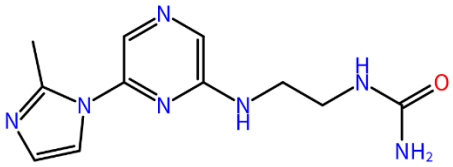	5.78
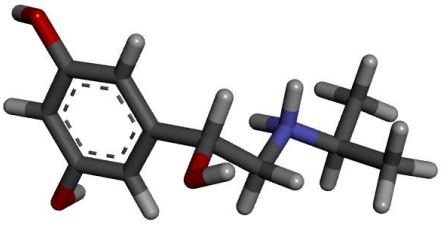 ZINC00002273	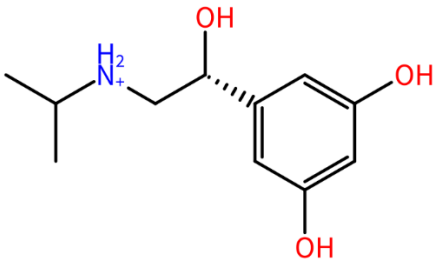	5.76
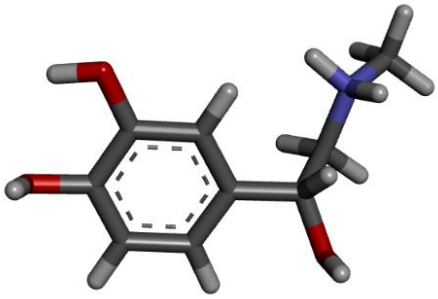 ZINC00039089	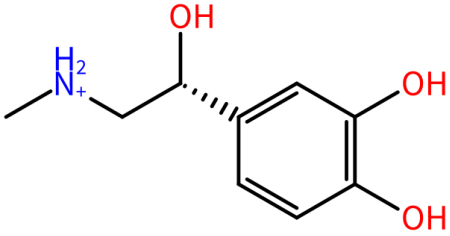	5.63

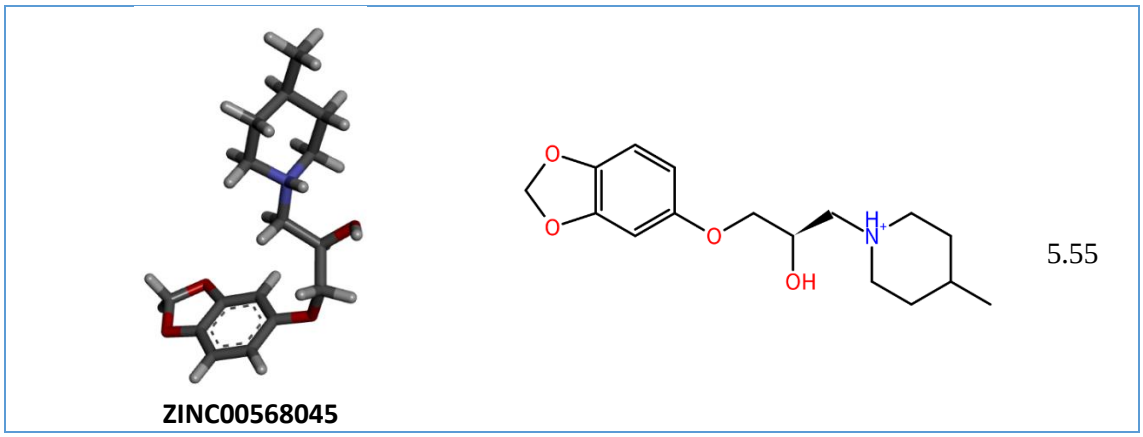

3.3 *De Novo* Growth

3.3.1 Topology Mapping

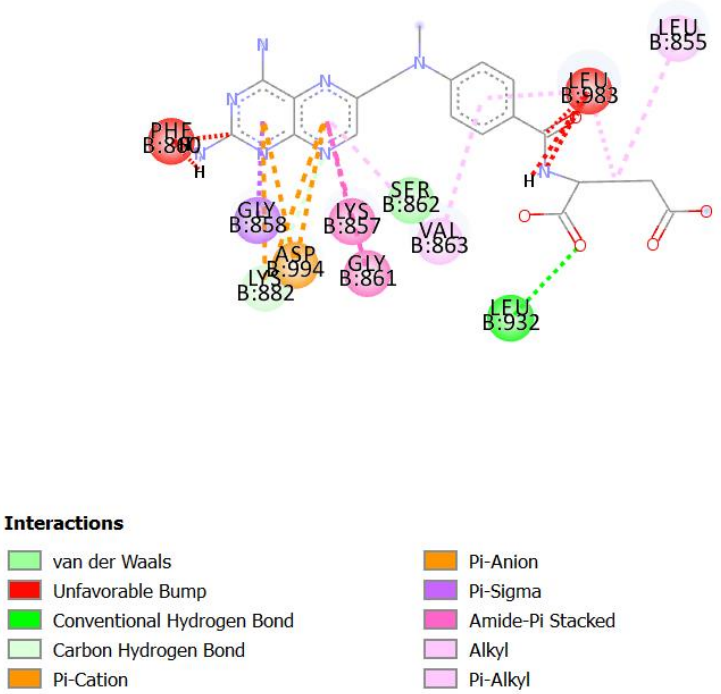

Figure 3.3: The 2D topology map indicating the critical interactions between the Methotrexate molecule and the amino acids lining the ligand binding pocket of JAK2, as described in PDB 2B7A (Lucet et al, 2005), rendered in Discovery Studio®[2]

[2] Dassault Systèmes. BIOVIA Discovery Studio Visualizer. Version 20.1 [Software]. San Diego: Dassault Systèmes; 2020 [cited 2021 Jul 26]. Available from URL: https://www.3dsbiovia.com/products/collaborative-science/biovia-discovery-studio/visualization-download.php

Figure 3.3 above depicted the important pharmacophoric moieties which were important for biological activity of the optimal MTX molecule within the JAK2 LBP. Therefore, the 2D topology map was used as a template in seed creation, since those moieties which were necessary for such activity were kept, and any unfavourable bumps were substituted with other atoms, to try and improve binding of the molecule and in turn the biological activity.

3.3.2 Ligand Binding Pocket Mapping

When carrying out the POCKET function on LigBuilder® v1.2 (Wang et al, 2000), a pharmacophore and a key site for the optimal MTX conformer was generated, as seen in Figures 3.4 and 3.5. The blue spheres represent hydrogen bond donors whilst the grey spheres represent hydrophobic grids. The red spheres denote hydrogen bond acceptors.

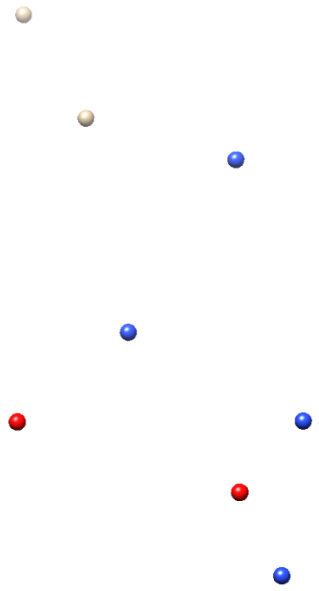

Figure 3.4: The pharmacophore for the optimal Methotrexate conformer generated using the POCKET module in LigBuilder® v1.2 (Wang et al, 2000), rendered in UCSF Chimera® v.1.12 (Petterson et al., 2004)

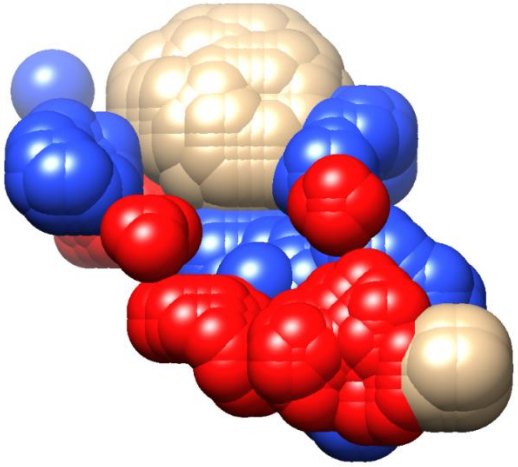

Figure 3.5: The key site for the optimal Methotrexate conformer generated using the POCKET module in LigBuilder® v1.2 (Wang et al, 2000), rendered in UCSF Chimera® v.1.12 (Petterson et al., 2004)

3.3.3 Seed Generation

Three modelled seeds were successfully grown within the JAK2 LBP. The H.spc atoms which are indicative of the growing sites are shown in white.

Table 3.3: The seed structures generated during the *De Novo* method, rendered in UCSF Chimera® v.1.12 (Petterson et al., 2004)

Seed number	Seed structure
1	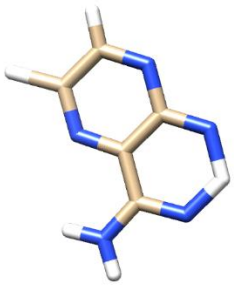 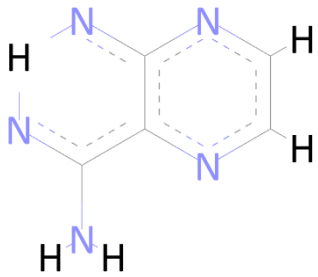
2	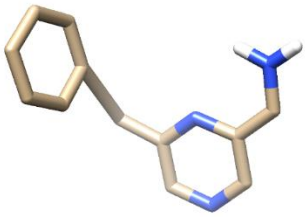 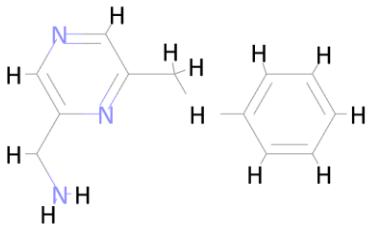
3	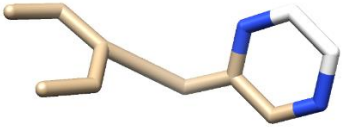 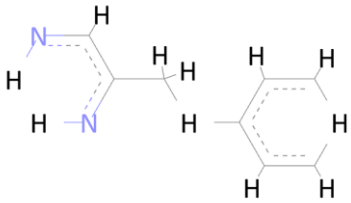

3.3.4 Ligands Generated by Structure-Based Drug Design

Seed 1 generated 200 ligands, seed 2 generated 20 ligands and seed 3 generated 7 ligands. These ligands were filtered and the best ligands were selected.

When seed 1 was filtered, none of the novel molecules were Lipinski rule (Lipinski et al, 2001) compliant since some had a MW of more than 500, others had a logP of more than 5 whilst some had more than 5 H-bond donors and 10 H-bond acceptors. Hence these molecules were eliminated since they are not preferred. This is because molecules with these properties are more likely to have poor absorption or permeation.

When seed 2 was filtered for Lipinski rule (Lipinski et al, 2001) compliance, 13 novel molecules remained out of the 20 initial ligands. Table 3.4 below shows these molecules according to the family they belong to. Different families have a different pharmacophore structure. The green box depicts the seed which was obtained through the fragmentation exercise of MTX. The red box shows the general pharmacophore.

Table 3.4: *De Novo* ligands obtained from Seed 2, rendered in UCSF Chimera® v.1.12 (Petterson et al, 2004)

Family 1	Properties
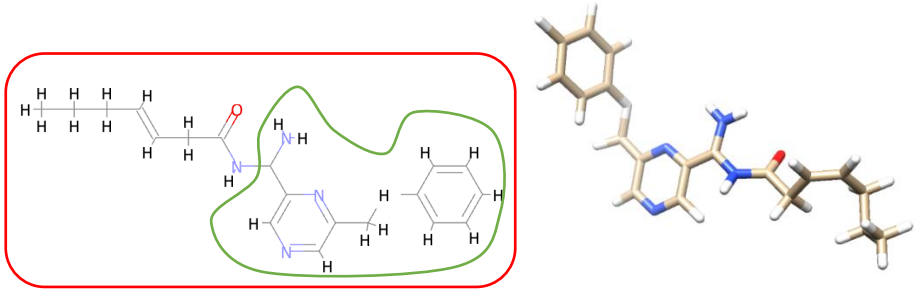 C19H24N4O	MW: 324 LogP: 3.85 pKd: 5.35 HBA: 4 HBD: 4
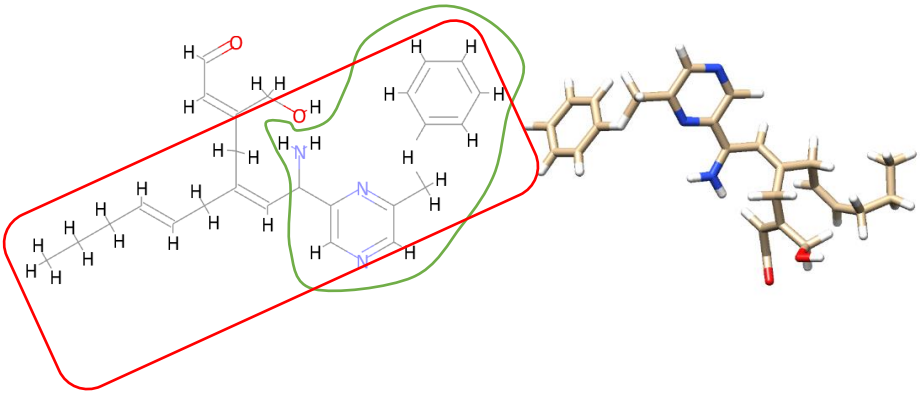 C25H31N3O2	MW: 405 LogP: 3.95 pKd: 5.09 HBA: 5 HBD: 4
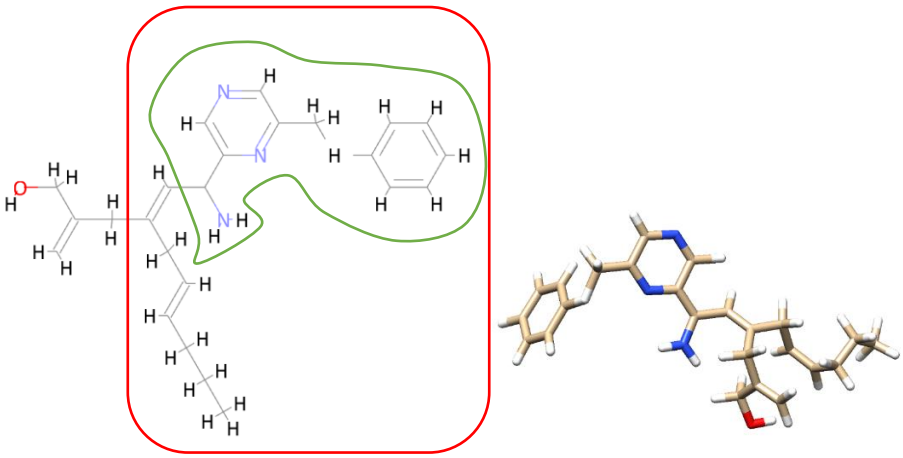 C24H31N3O	MW: 377 LogP: 4.5 pKd: 5.73 HBA: 4 HBD: 4

Family 2	
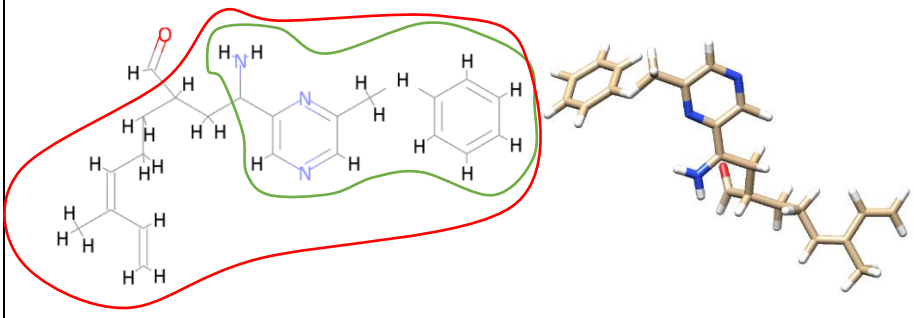 C22H27N3O	MW: 349 LogP: 4.64 pKd: 5.16 HBA: 4 HBD: 3
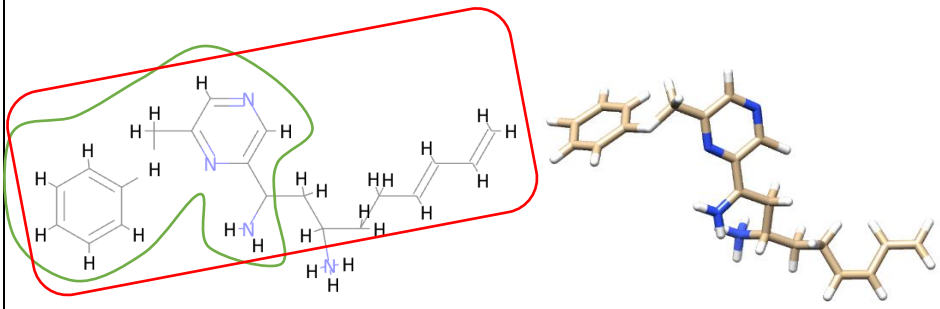 C20H27N4	MW: 323 LogP: 3.51 pKd: 5.95 HBA: 3 HBD: 4
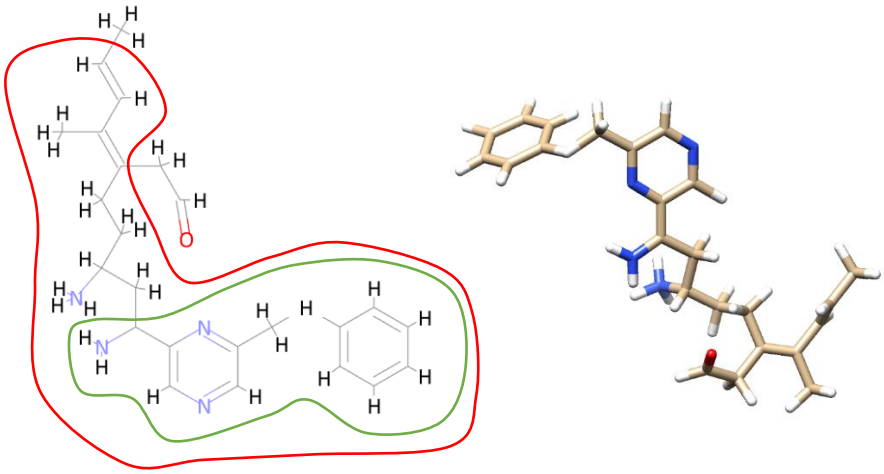 C24H33N4O	MW: 393 LogP: 3.65 pKd: 5.92 HBA: 4 HBD: 4

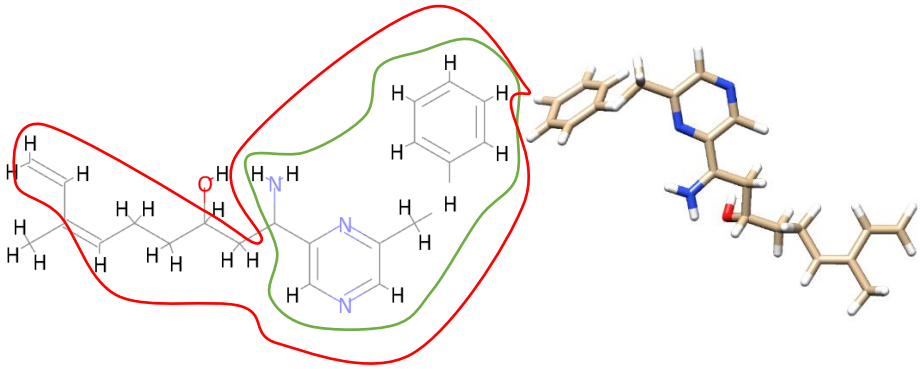 C21H27N30	MW: 337 LogP: 3.93 pKd: 6.09 HBA: 4 HBD: 4
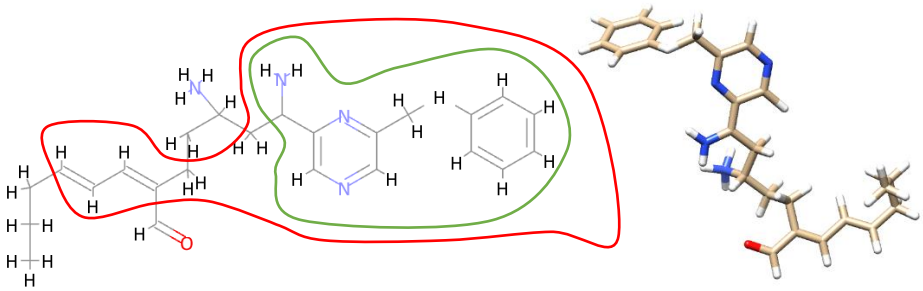 C24H33N4O	MW: 393 LogP: 3.93 pKd: 5.4 HBA: 4 HBD: 4
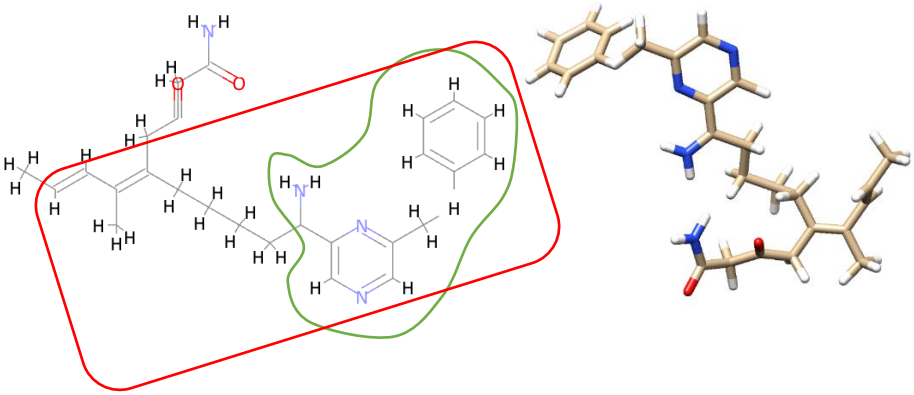 C26H34N402	MW: 434 LogP: 4.07 pKd: 5.28 HBA: 5 HBD: 4

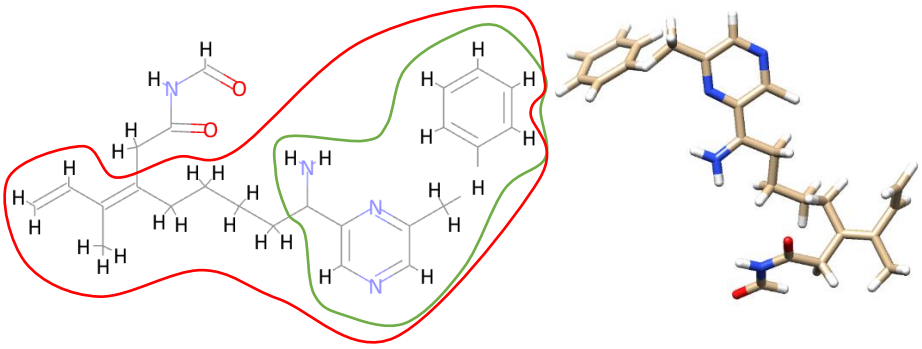 C24H30N4O2	MW: 406 LogP: 4.23 pKd: 5.31 HBA: 5 HBD: 4
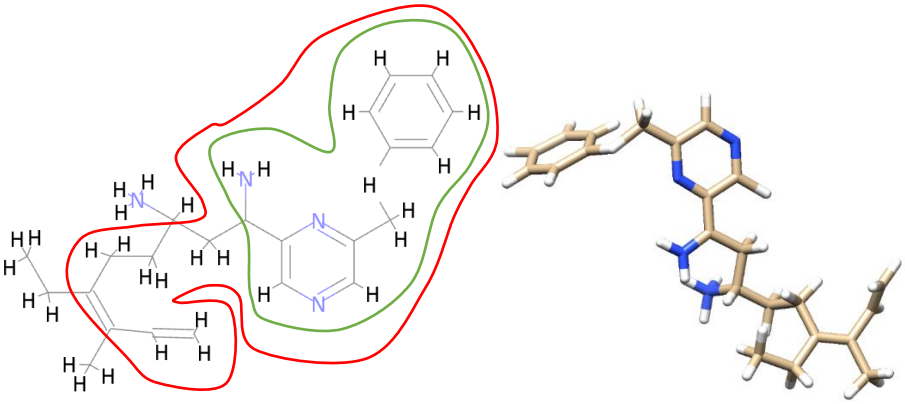 C23H33N4	MW: 365 LogP: 4.39 pKd: 5.55 HBA: 3 HBD: 4
Family 3	
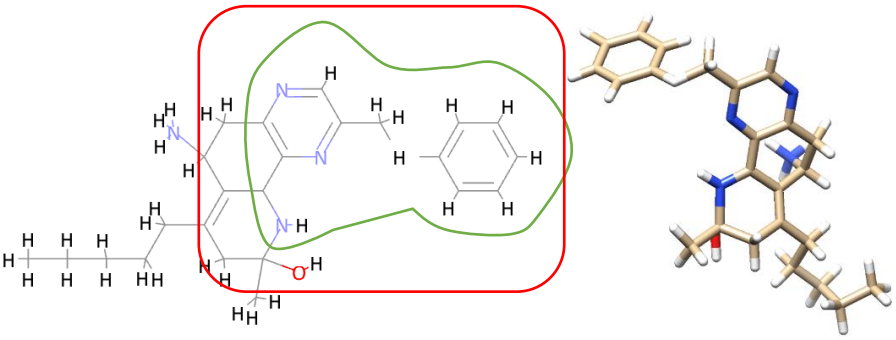 C24H33N4O	MW: 393 LogP: 4.05 pKd: 5.07 HBA: 4 HBD: 5

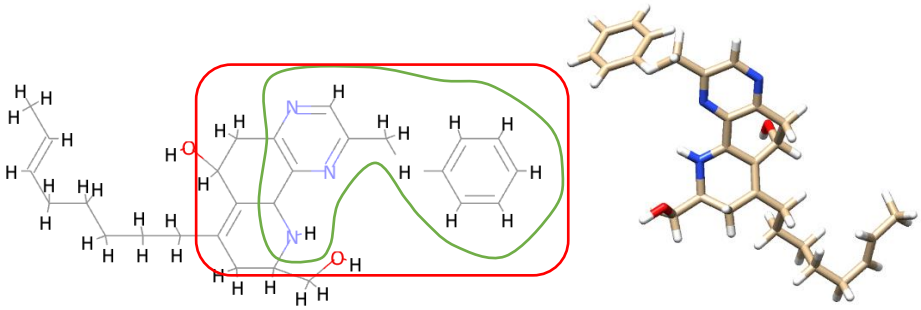 C27H35N302	MW: 433 LogP: 4.86 pKd: 5.39 HBA: 5 HBD: 5

From seed 3, 6 novel molecules out of 7 remained following the filtering process as can be seen in Table 3.5. The green box depicts the seed structure on which the novel molecule was built, whilst the red box depicts the pharmacophore which changes from one family to the other. Some families within this seed only had one molecule, hence their pharmacophoric structure could not be identified.

Table 3.5: *De Novo* ligands obtained from Seed 3, rendered in UCSF Chimera® v.1.12 (Petterson et al, 2004)

Family 1	Properties
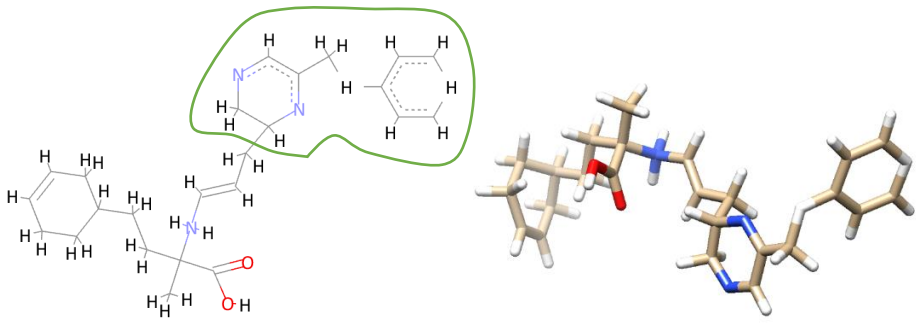 C24H35N3O2	MW: 397 LogP: 4.53 pKd: 5.44 HBA: 4 HBD: 2

Family 2	
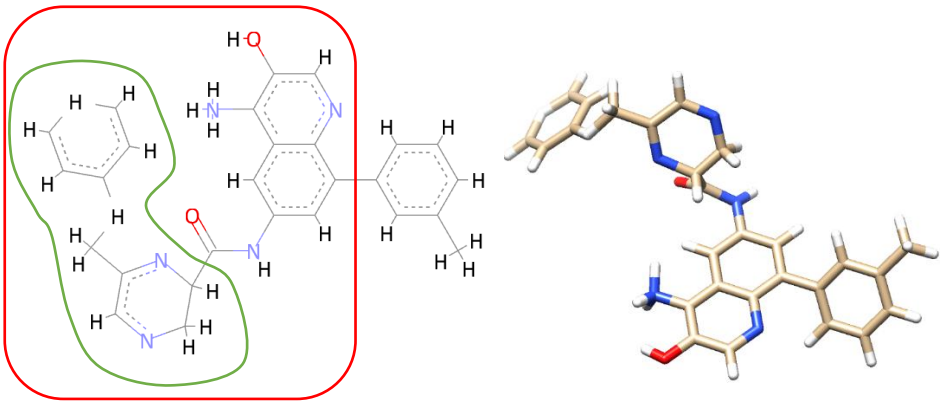 C27H27N5O2	MW: 453 LogP: 3.35 pKd: 5.37 HBA: 5 HBD: 3
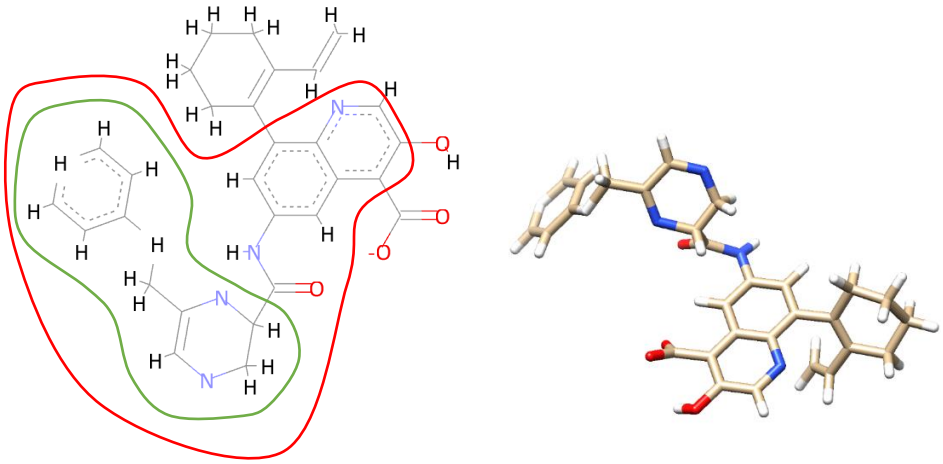 C29H28N4O4	MW: 496 LogP: 3.68 pKd: 5.03 HBA: 7 HBD: 3
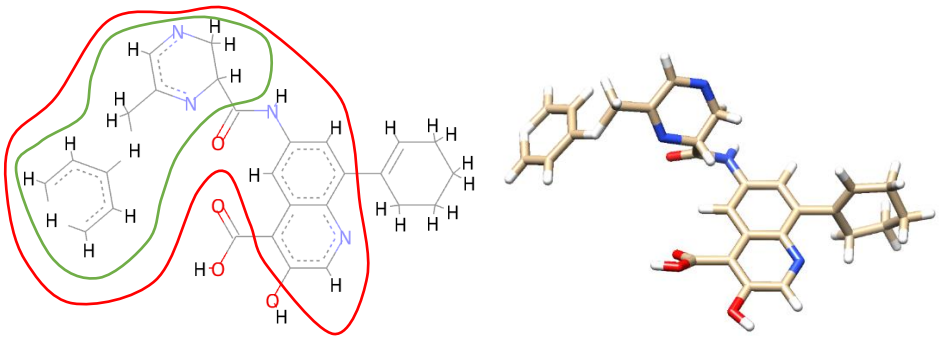 C27H27N4O4	MW: 471 LogP: 4.15 pKd: 5.22 HBA: 7 HBD: 3

Family 3	
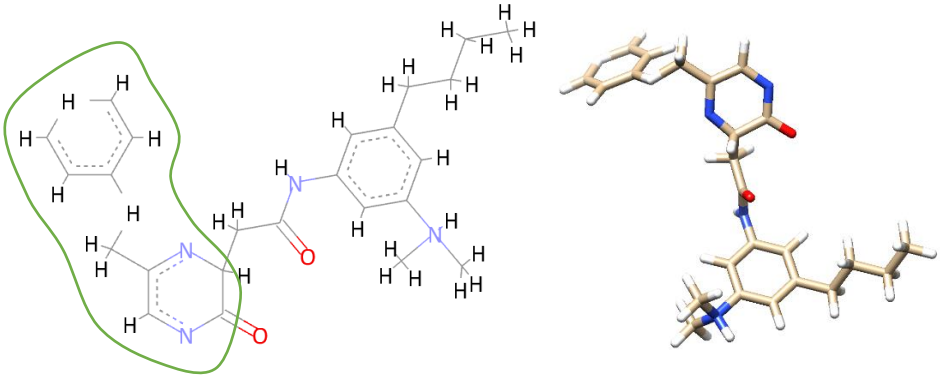 C24H32N4O2	MW: 408 LogP: 3.69 pKd: 5.09 HBA: 4 HBD: 2
Family 4	
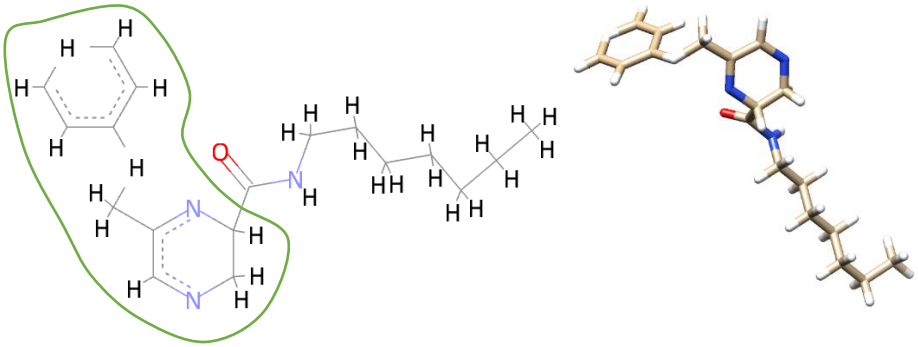 C18H28N3O	MW: 302 LogP: 3.16 pKd: 5.09 HBA: 3 HBD: 1

3.3.5 Identification of the Highest Affinity *De Novo* Generated Molecules

The molecule with the highest affinity (pKd) was considered to be one of the best molecules. For each of the seeds, the best molecules were chosen.

Table 3.6: The top 3 molecules generated from Seed 2 and their properties. Images rendered in Discovery Studio®[2]

Molecule Number	Family	2D Structure	MW	LogP	pKd	HBA	HBD
8	<2>	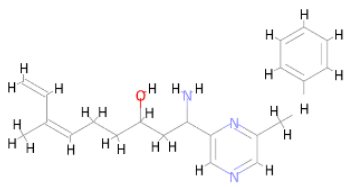	337	3.93	6.09	4	4
9	<2>	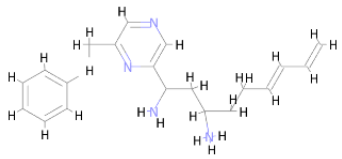	323	3.51	5.95	3	4
10	<2>	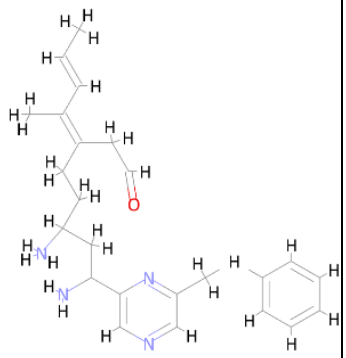	393	3.65	5.92	4	4

[2] Dassault Systèmes. BIOVIA Discovery Studio Visualizer. Version 20.1 [Software]. San Diego: Dassault Systèmes; 2020 [cited 2021 Jul 26]. Available from URL: https://www.3dsbiovia.com/products/collaborative-science/biovia-discovery-studio/visualization-download.php

Table 3.7: The top 3 molecules generated from Seed 3 and their properties. Images rendered in Discovery Studio®[2]

Molecule Number	Family	2D Structure	MW	LogP	pKd	HBA	HBD
1	<1>	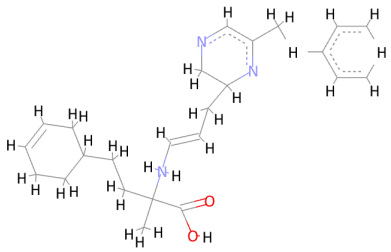	397	4.53	5.44	4	2
2	<2>	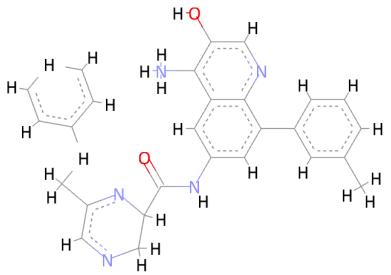	453	3.35	5.37	5	3
3	<2>	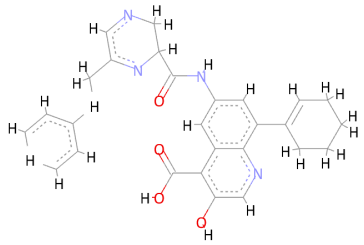	471	4.15	5.22	7	3

[2] Dassault Systèmes. BIOVIA Discovery Studio Visualizer. Version 20.1 [Software]. San Diego: Dassault Systèmes; 2020 [cited 2021 Jul 26]. Available from URL: https://www.3dsbiovia.com/products/collaborative-science/biovia-discovery-studio/visualization-download.php

Chapter 4

Discussion

4.1 Rationale for the Study

Literature shows that driver mutations in the *JAK2V617F* gene lead to the activation of the JAK/STAT signalling pathway, and to MPNs, through the initiation of erythrocytosis and a number of inflammatory responses. Antagonism of the JAK/STAT signalling pathway can reverse this underlying marrow pathology by disrupting erythrocytosis, indicating that JAK2 represents a viable target for mitigation of the progression of MPNs (Chinnaiya et al, 2017). A number of potential molecules which have JAK inhibition properties have undergone testing for their possible indication in MPNs, however, only a few have been successful, primarily because of toxicity issues (Verstovsek & Bose, 2017).

Studies have shown that low-dose MTX binds to JAK2 with high affinity, making its scaffold useful for the identification of analog molecules (Chinnaiya et al, 2017). This is important from a drug repurposing perspective since when drugs are repurposed, there is significant information that is already known with regards to their *in vivo* disposition, bioavailability, pharmacokinetics and adverse effect profile. Therefore time is gained, less failures are expected in what is usually associated with drug discovery, and the process is less expensive than having to start all research from scratch (March-Vila et al, 2017).

Based on this evidence, JAK2 was selected as the target and MTX was chosen as the lead molecule. From a drug design perspective, the choice of MTX as the lead molecule can be facilitated by the fact that this molecule is already on the market. A computational drug repurposing approach is a worthwhile approach to find new indications for drugs which are already approved for other indications and are already available on the market.

Repurposed drugs have a lower risk of failure since their safety in humans is already long-established.

This study tackled two different drug design approaches: *de novo* and VS. Both VS and the *de novo* approach have similar aims. Their main aim is to identify a number of molecules that have a biological activity towards a specific target. The approach which is taken is usually dependent on the data that is available on the known ligand as well as information on the 3D structure of the target protein (Douguet, 2010).

4.2 Analysis of Results of the Virtual Screening Approach

In the VS approach, crystallographic deposition PDB 2B7A (Lucet et al, 2006), describing the bound co-ordinates of JAK2 in complex with the pan-JAK inhibitor tetracyclic pyridone-6, was used. The MTX molecule, which was sketched on SYBYL®-X 1.1 (Ash et al, 2010) was also used. A pharmacophore for both the tetracylic pyridone and the MTX molecule was generated and the critical interactions forged by the bioactive conformers were analysed and modelled in LigandScout® (Wolber & Langer, 2005). The two pharmacophores were superimposed and a unique average pharmacophore was generated. This pharmacophore was then used as a query on the online database ZincPharmer® (Koes & Camacho, 2012), where filters for the hit molecules, whose electronic and spatial arrangements were analogous to the modelled pharmacophore, were identified. Filters were applied to ensure lead-like nature of the identified hits, according to the Rule of 3 (Congreve et al, 2003). A second filtration process was then carried out in MONA® (Hilbig & Rarey, 2015), where hit molecules were filtered according to Lipinski's rule of 5 (Lipinski et al, 2001). The remaining 991 hit molecules were docked

into a generated protomol and ranked according to their affinity for the JAK2 LBP. This led to the identification of the optimal structures.

In this case, LBA is determined by the total score, as opposed to the pKd. A hit molecule with a high total score suggested that the ligand established more favourable interactions with the JAK2 LBP. The 3 hit structures with the highest affinity for the modelled protomol were identified, and selected for recommendation for further validation and optimisation.

As a first step in this process, these molecules were guided into the JAK2 LBP, docked, and conformational analysis performed. The optimal conformer of each hit structure within the JAK2 LBP, and 2D topology maps were generated to facilitate visualization of the critical interactions that were forged with the JAK2 LBP. Since the hit molecules generated did not have a common molecular structure, it was evident that the interactions forged between the hit molecules and the JAK2 LBP differed from one another with respect to the positioning of the molecule. It was interesting to note however, that in most cases, the amino acids involved in ligand binding within the JAK2 LBP were conserved.

4.2.1 Analysis of ZINC00034158

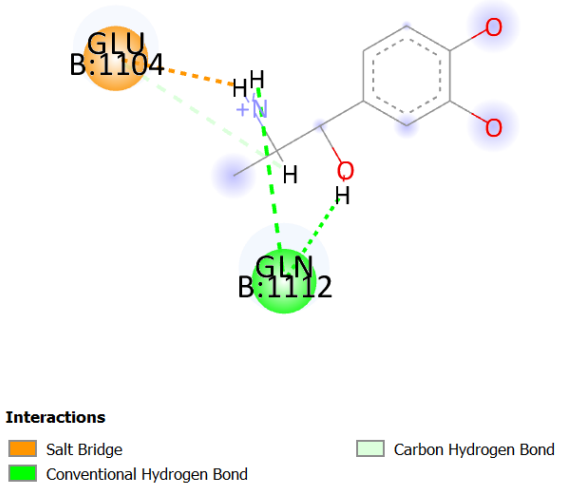

Figure 4.1: The 2D topology map indicating the ligand-receptor interactions between ZINC00034158 and the amino acids lining the ligand binding pocket of JAK2 as described in PDB 2B7A (Lucet et al, 2005) rendered in Discovery Studio®[2]

The positively charged primary amine on ZINC00034158 (Figure 3.2) forged interactions with 2 amino acid residues lining the JAK2 LBP, a salt bridge and a hydrogen bond, with Glu^{1104} and GLN^{1112} respectively. GLN^{1112} also interacted with a hydroxyl group. The fact that there were no unfavourable bumps, notably aided in an improved affinity. The benzene ring in the molecule forged no critical interactions with the LBP, therefore it was not important for binding.

[2] Dassault Systèmes. BIOVIA Discovery Studio Visualizer. Version 20.1 [Software]. San Diego: Dassault Systèmes; 2020 [cited 2021 Jul 26]. Available from URL: https://www.3dsbiovia.com/products/collaborative-science/biovia-discovery-studio/visualization-download.php

4.2.2 Analysis of ZINC92898345

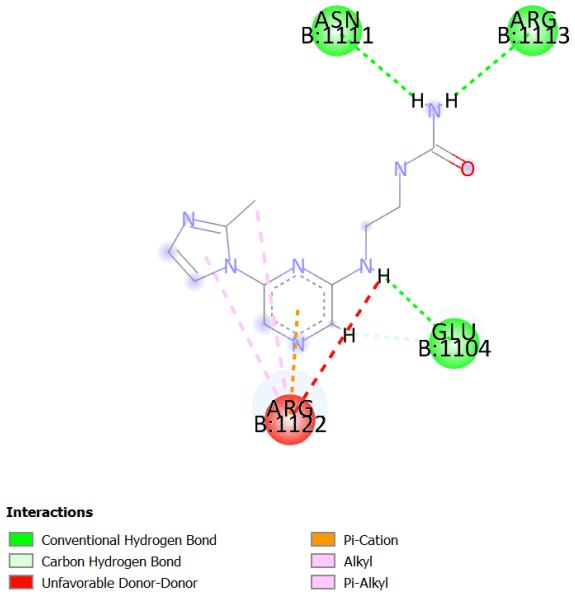

Figure 4.2: The 2D topology map indicating the ligand-receptor interactions between ZINC92898345 and the amino acids lining the ligand binding pocket of JAK2 as described in PDB 2B7A (Lucet et al, 2005) rendered in Discovery Studio®[2]

An unfavourable donor- donor interaction was observed between an amino group and the amino acid Arg^{1122} within the LBP. This could be attributed to the fact that the affinity of this molecule for the JAK2 receptor was lower than that with ZINC00034158 (Figure 3.2), which had no unfavourable bumps which could confer instability. The same amino group also formed a hydrogen bond with the amino acid Glu^{1104}. This molecule formed a total of three conventional hydrogen bonds with amino acids Glu^{1104}, Asn^{1111} and Arg^{1113}.

[2] Dassault Systèmes. BIOVIA Discovery Studio Visualizer. Version 20.1 [Software]. San Diego: Dassault Systèmes; 2020 [cited 2021 Jul 26]. Available from URL: https://www.3dsbiovia.com/products/collaborative-science/biovia-discovery-studio/visualization-download.php

4.2.3 Analysis of ZINC00002273

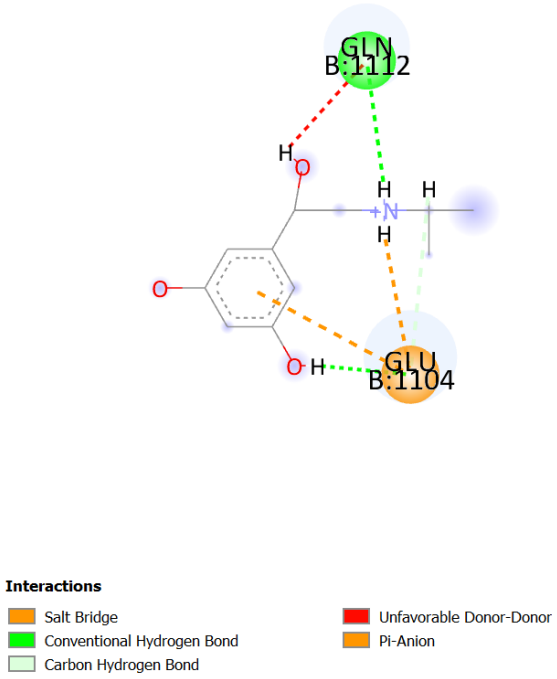

Figure 4.3: The 2D topology map indicating the ligand-receptor interactions between ZINC00002273 and the amino acids lining the ligand binding pocket of JAK2 as described in PDB 2B7A (Lucet et al, 2005) rendered in Discovery Studio®[2]

An unfavourable donor-donor interaction arose between the hydroxyl group in the molecule and the GLN^{1112} amino acid within the JAK2 LBP, inferring instability, which could have contributed to the reduced affinity. The primary amine group in the ZINC00002273 (Figure 3.2) seems to be important for binding since it forged interactions with two amino acids lining the JAK2 LBP. In fact, it formed a salt bridge with Glu^{1104} and a conventional hydrogen bond with GLN^{1112}. Another salt bridge was evident between Glu^{1104} and the substituted benzene ring. The hydroxyl group on the benzene ring also contributed to a hydrogen bond with Glu^{1104}.

[2] Dassault Systèmes. BIOVIA Discovery Studio Visualizer. Version 20.1 [Software]. San Diego: Dassault Systèmes; 2020 [cited 2021 Jul 26]. Available from URL: https://www.3dsbiovia.com/products/collaborative-science/biovia-discovery-studio/visualization-download.php

4.2.4 Comparison of the Highest-Ranking Virtual Screening Molecule to the Optimal Methotrexate Conformer

Bulkiness of a molecule plays an important role to ligand binding and affinity since simpler molecules tend to bind with more affinity. It was evident in this case that the MTX molecule is much bulkier than ZINC00034158 (Figure 3.2), hence the greater affinity of the VS generated molecule when compared to MTX. Moreover, ZINC00034158 (Figure 3.2) had no unfavourable bumps between the molecule and the JAK2 LBP which could impact negatively its affinity. This is not the case with the MTX molecule that had five unfavourable bumps in its structure. Phe^{860} contributed to two of these bumps, one with a hydrogen atom on the benzene ring and the other with a hydrogen atom attached to a nitrogen atom. Leu^{983} was also a contributor to three unfavourable bumps. Two of these bumps were with both atoms of an amine group and one with a carbon atom.

4.3 Analysis of Results of the *De Novo* Approach

In the *de novo* approach, a 2D topology map, that highlighted the interactions between the optimal MTX conformer and the JAK2 LBP, was used to identify the fundamental atoms required for this interaction to occur. This aided in the creation of high efficiency seeds through a fragmentation exercise. These small molecules were docked within the bioactive binding site that was generated using the pocket module in LigBuilder® v1.2 (Wang et al, 2000). *De novo* growth was performed in non-critical loci to ensure optimal interaction within the LBP. The novel structures generated were filtered according to Lipinski Rule compliance (Lipinski et al, 2001), grouped into families according to

pharmacophoric similarities and the optimal structures chosen on the basis of affinity for the JAK2 LBP.

4.3.1 Analysis of the Highest Affinity *De Novo* Generated Molecule

When the novel molecules for the three seeds generated were filtered, most of them were not Lipinski Rule (Lipinski et al, 2001) compliant, hence they were eliminated. Therefore, the pool of novel molecules decreased significantly (n = 19). This led to the optimal molecules being chosen based on their affinity for the JAK2 LBP. The optimal *de novo* structure derived from Seed 2 and had an affinity of 6.09 (pKd). This affinity is lower than that of the bound tetracyclic pyridone to JAK2, which had an affinity of 6.85 (pKd). Upon comparing the binding affinity with that of the optimal MTX conformer, which had an affinity of 5.81 (pKd), the best molecule still had a better affinity.

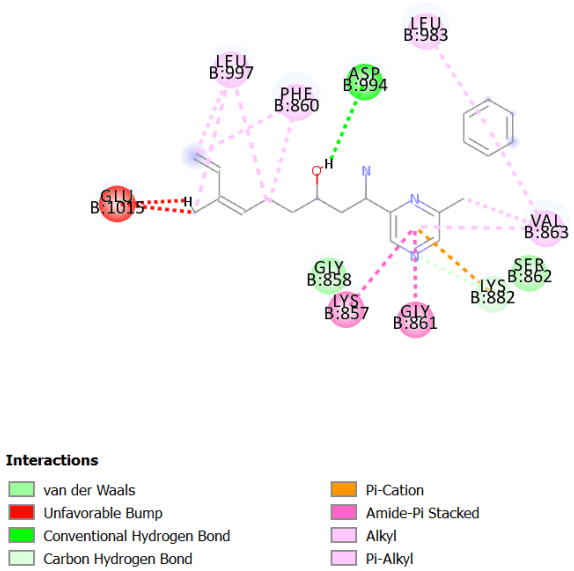

Figure 4.4: The 2D topology map indicating the ligand-receptor interactions between the highest affinity molecule of Seed 2 and the amino acids lining the ligand binding pocket of JAK2 as described in PDB 2B7A (Lucet et al, 2005) rendered in Discovery Studio®[2]

The high binding affinity of this molecule with the LBP of JAK2 could be attributed to the large number of hydrophobic interactions that surround the molecule, hence increasing its stability within the JAK2 LBP, and in turn leading to a higher binding affinity. The presence of a number of alkyl interactions increased the hydrophobicity of the molecule. Alky interactions occured with Leu^{997}, Phe^{860}, Leu^{983} and Val^{863}. Only one unfavourable bump was present between Glu^{1015} and a hydrogen. A hydrogen bond between Asp^{994} and the hydroxyl group on the molecule further stabilized the interaction with the LBP. An interaction between the nitrogen atom on the benzene ring and Lys^{882} was a further contributor to binding.

[2] Dassault Systèmes. BIOVIA Discovery Studio Visualizer. Version 20.1 [Software]. San Diego: Dassault Systèmes; 2020 [cited 2021 Jul 26]. Available from URL: https://www.3dsbiovia.com/products/collaborative-science/biovia-discovery-studio/visualization-download.php

4.3.2 Comparison of the Best Generated *De Novo* Molecule to the Optimal Methotrexate Conformer

When comparing the topology map of the optimal MTX conformer to the JAK2 LBP with that of the best *de novo* generated molecule to the JAK2 LBP, it is evident that the former has a higher number of unfavourable bumps, which could be a contributor to the reduced affinity when compared to the *de novo* generated molecule. Moreover, the MTX molecule is bulkier, with more benzene rings. In fact, the *de novo* generated molecule has a MW of 337 whilst MTX has a MW of 454. This could have also attributed to the lower binding affinity on comparison with the *de novo* generated molecule.

4.4 Identification of the Amino Acids Critical to Binding

The identification of the amino acids within a receptors' LBP which are necessary for binding with a molecule is an important step in the understanding of how a specific molecule binds to it. When comparing the MTX and JAK2 LBP topology map with those of the top 3 hit molecules generated through VS and the best novel molecule obtained from the *de novo* approach, the common amino acids which had critical interactions with each molecule were recorded.

Graph 4.1: A graph of the common critical amino acids necessary for binding with the JAK2 ligand binding pocket vs frequency

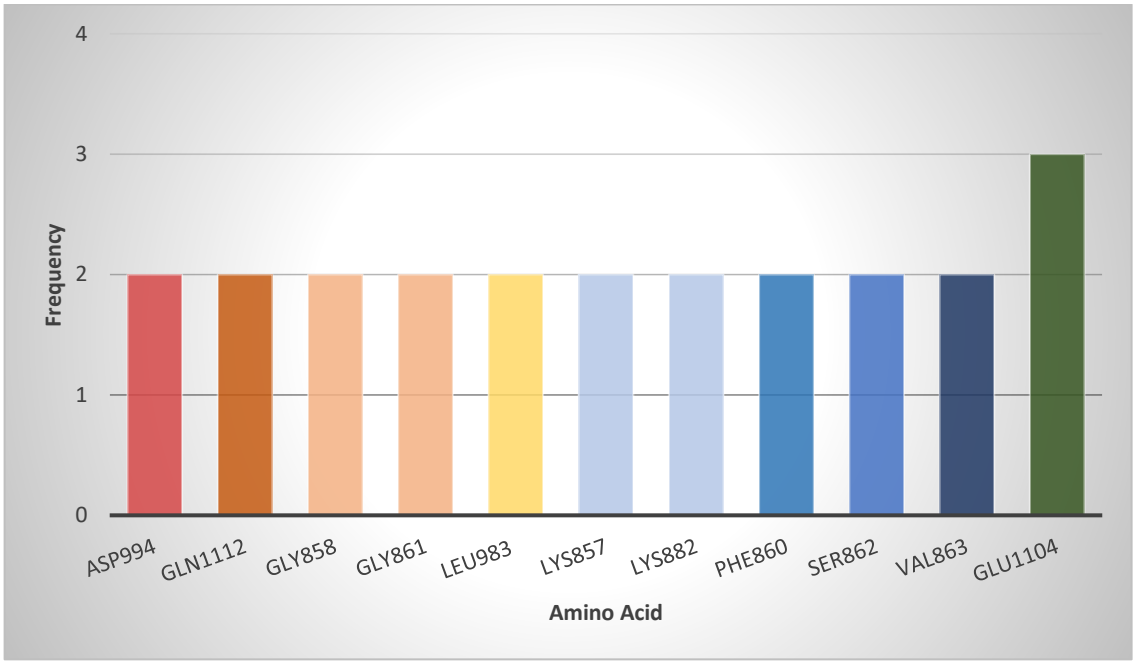

As can be seen in Graph 4.1 above, the amino acid Glu^{1104} seems to be the most critical to binding. Interactions with this amino acid appeared with all the Virtual Screening generated molecules. It is also evident that the best affinity molecule generated through the *de novo* approach has more interactions forged with the same amino acids as the MTX molecule. The common amino acids which seem important for binding between these two molecules included Leu^{983}, Asp^{994}, Phe^{860}, Gly^{858}, Lys^{857}, Gly^{861}, Lys^{882}, Ser^{862}, Val^{863}. Therefore, when designing a new molecule for binding with the JAK2 LBP, it is crucial to make sure that it contains moieties which are able to forge interactions with these amino acids.

4.5 Comparison of *De Novo* and Virtual Screening

VS employs a number of steps including molecular docking and ligand similarity, as explored in this study (Jang et al, 2021). During the VS process, robust databases that contain 3D structures of molecules are computationally evaluated. These molecules are filtered and the most promising ones are selected. VS aims at choosing those hit molecules which have the best LBA (pKd) to the target protein, and therefore only the most promising molecules with biological activity against the target of interest are synthesized. VS is also able to identify those moieties which might not be favourable, therefore in the end, this method aids in the identification of new and bioactive molecules. VS can be divided into two: structure-based VS and ligand-based VS. In this study, ligand-based VS was used. In this form of VS, a lead molecule or its pharmacophore is used to query a database in order to identify structurally analogous hit structures. In this study, an average or consensus pharmacophore comprising the critical interactions of MTX and pyridone-6 was the modelled query structure (Maia et al, 2020). On the other hand, structure-based VS uses the information that is known about the ligand binding pocket of a target receptor rather than the structure of the lead molecule. This method is only opted for when no lead molecule structure is available (Hamza et al, 2012).

During the *de novo* approach, the modelled seeds were docked into a pharmacophoric space which was already described crystallographically and known to be bioactive. Hence, the *de novo* generated molecules had a higher propensity to bioactivity. Moreover, the seed molecules could be said to be high efficiency molecules since they incorporated those moieties which were the most critical to binding in MTX. However, this approach does not lead to significant structural innovation. This is because the designed seeds structures, which formed the primary pharmacophoric structure, were user modelled.

It must also be pointed out that in the case of the VS structures, these are already present on the ZincPharmer® (Koes & Camacho, 2012) database in a purchasable form, which eliminates the necessity of synthesis from the first optimisation stage of the study. The same cannot be said for the *de novo* designed molecules, for which a synthetic pathway must often be devised.

4.6 Conclusion

By adopting this dual approach, complementarity was achieved. The VS approach provided the advantage of using a robust probe, which was a non-restrictive pharmacophore, to elucidate the JAK2 LBP and generate a pharmacophoric structure for ligands of this LBP. Even though these molecules were pharmacophorically similar to the protomol, they were structurally diverse to the lead molecule. The use of the Rule of 3 (Congreve et al, 2003) criteria for filtration of hit molecules from a MW perspective and from a rotatable bond perspective, leaves sufficient room for the introduction of new molecules during the process of optimisation, increasing innovation. One short-coming of the VS approach is that since the molecules were then docked into the protomol, the propensity towards bioactivity was reduced. This shortcoming was however overcome through the *de novo* approach.

The optimal structures obtained from both approaches will be compared from an atomic perspective and further validated for clinical usefulness through molecular dynamics simulation studies.

In this study, the lead molecule was MTX, an old drug, about which there is significant information from both a pharmacokinetic and a toxicological perspective. In this study,

the molecules derived from VS do not contain the MTX scaffold, and consequently require meticulous study from these perspectives. In the case of the *de novo* designed structures, the fact that these bear to different extents, significant portions of the MTX skeleton could perhaps decrease the risk of unfavourable adverse effects and unacceptable pharmacokinetics. The reality is however that sometimes even very small structural modifications to a molecule could impact significantly both toxicity and bioavailability. This means that even for the *de novo* designed molecular cohort attention should be given to establishing their pharmacokinetic and toxicity profile.

4.7 Limitations

A major limitation of this study is that *in silico* drug design is restricted, due to the rigid conditions that the study is conducted in, hence, it is not a true representation of the *in vivo* scenario. This leads to a less robust hypothesis with respect to the way with which the molecules will behave in the *in vivo* scenario. In addition, future *in vitro* studies carried out might render the molecules irrelevant through the discovery and detection of certain specific biological functions.

References

Alexander SPH, Fabbro D, Kelly E, Mathie A, Peters JA, Veale EL, et al. The Concise Guide To Pharmacology 2019/20: Enzymes. British Journal of Pharmacology. 2019;176(S1):S297-S396.

Ash S, Cline MA, Homer RW, Hurst T, Smith GB. ChemInform. 2010;28(18):66-78.

Barbui T, Barosi G, Birgegard G, Cervantes F, Finazzi G, Griesshammer M, et al. Philadelphia-Negative Classical Myeloproliferative Neoplasms: Critical Concepts and Management Recommendations From European LeukemiaNet. Journal of Clinical Oncology. 2011;29(6):761-770.

Berman HM, Westbrook J, Feng Z, Gilliland G, Bhat TN, Weissig H, et al. The Protein Data Bank. Nucleic Acids Research. 2000; 28:235-242.

Chinnaiya K, Lawson MA, Thomas S, Haider M-T, Down J, Chantry AD, et al. Low-dose methotrexate in myeloproliferative neoplasm models. Haematologica. 2017;102:336-339.

Congreve M, Carr R, Muray C, Jhoti H. A 'rule of three' for fragment-based lead discovery?. Drug Discovery Today. 2003; 8(19):876-877.

De Vos AM, Ultsch M, Kossiakoff AA. Human growth hormone and extracellular domain of its receptor: crystal structure of the complex. Science. 1992;255(5042):306-312.

Devos T, Beguin Y, Noens L, Van Eygen K, Zachée P, Mineur P, et al. Disease and treatment chaFracteristics of polycythemia vera patients in Belgium: Results from a scientific survey. European Journal of Haematology. 2017;100(4):361-366.

Douguet D. e-LEA3D: a computational-aided drug design web server. Nucleic Acids Research. 2010; 38(2): W615-W621.

Fan CM, Foster BK, Hui SK, Xian CJ. Prevention of Bone Growth Defects, Increased Bone Resorption and Marrow Adiposity with Folinic Acid in Rats Receiving Long-Term Methotrexate. Public Library of Science [Internet]. 2012;7(10):e46915 [cited 2020 May 02]. Available from URL: https://www.ncbi.nlm.nih.gov/pmc/articles/PMC3465278/

Fiehn C. A new weapon against an old target. Arthritis Research & Therapy. 2011;13(4):122.

Finazzi G, Barbui T. The treatment of polycythaemia vera: an update in the JAK2 era. Internal and Emergency Medicine. 2007;2(1):13-18.

Francis S, Thomas S, Luben R, Sousos N, Mead A, Snowden JA, et al. Low-dose methotrexate: potential clinical impact on haematological and constitutional symptoms in myeloproliferative neoplasms. British Journal of Haematology. 2019;187(3):e69-e72.

Geyer HL, Mesa RA. Therapy for myeloproliferative neoplasms: when, which agent, and how?. Blood. 2014;124:3529-3537.

Goerttler P, Kreutz C, Donauer J, Faller D, Maiwald T, Marz E, et al. Gene expression profiling in polycythaemia vera: overexpression of transcription factor NF-E2. British Journal of Haematology. 2005;129(1):138-150.

Grinfeld J, Godfrey A. After 10 years of JAK2V617F: Disease biology and current management strategies in polycythaemia vera. Blood Reviews. 2017;31(3):101-118.

Hamza A, Wei NN, Zhan CG. Ligand-Based Virtual Screeing Approach Using a New Scoring Function. Journal of chemical information and modeling. 2012; 52(4): 963-974.

Hasselbalch HC, Holmström MO. Perspectives on interferon-alpha in the treatment of polycythemia vera and related myeloproliferative neoplasms: minimal residual disease and cure?. Seminars in Immunopathology. 2019; 41(1):5-19.

He R, Greipp P, Rangan A, Mai M, Chen D, Reichard K, et al. BCR–JAK2 fusion in a myeloproliferative neoplasm with associated eosinophilia. Cancer Genetics. 2016;209(5):223-228.

Hilbig M, Rarey M. MONA 2: A Light Cheminformatics Platform for Interactive Compound Library Processing. Journal of Chemical Information and Modeling. 2015;55(10):2071–2078.

Ioannidis S, Lamb ML, Wang T, Almeida L, Block MH, Davies AM, et al. Discovery of 5-Chloro-N2-[(1S)-1-(5-Fluoropyrimidin-2-Yl)Ethyl]-N4-(5-Methyl-1H-Pyrazol-3-Yl)Pyrimidine-2,4-Diamine (Azd1480) as a Novel Inhibitor of the Jak/Stat Pathway. Journal of Medicinal Chemistry. 2011;54 (1): 262–276.

Jain AN. Effects of Protein Conformation in Docking: Improved Pose Prediction through Protein Pocket Adaptation. Journal of Computer-Aided Molecular Design. 2009;23(6):355–374.

Jang WD, Jeon S, Kim S, Lee SY. Drugs repurposed for COVID-19 by virtual screening of 6,218 drugs and cell-based assay. National Academy of Sciences. 2021; 118(30): e2024302118

Joint Formulary Committee. British National Formulary (BNF). 72nd ed. London; BMJ Group and Pharmaceutical Press; 2016. p.807.

Kaserer T, Beck KR, Akram M, Odermatt A, Schuster D. Pharmacophore Models and Pharmacophore-Based Virtual Screening: Concepts and Applications Exemplified on Hydroxysteroid Dehydrogenases. Molecules. 2015:20:22799–22832.

Koes D, Camacho C. ZINCPharmer: pharmacophore search of the ZINC database. Nucleic Acids Research. 2012;40(1):409-414.

Kontoyianni M. Docking and Virtual Screening in Drug Discovery. Methods in Molecular Biology. 2017;1647:255-266.

Kurzer J, Argetsinger L, Zhou Y, Kouadio J, O'Shea J, Carter-Su C. Tyrosine 813 Is a Site of JAK2 Autophosphorylation Critical for Activation of JAK2 by SH2-B. Molecular and Cellular Biology. 2004;24(10):4557-4570.

Lipinski CA, Lombardo F, Dominy BW, Feeney PJ. Experimental and computational approaches to estimate solubility and permeability in drug discovery and development settings. Advanced Drug delivery Reviews. 2001;46(1-3):3-26.

Lucet IS, Fantino E, Styles M, Bamert R, Patel O, Broughton SE, et al. The structural basis of Janus kinase 2 inhibition by a potent and specific pan-Janus kinase inhibitor. Blood. 2005; 107: 176-183.

Maia EHB, Assis LC, de Oliveira TA, da Silva AM, Taranto AG. Structure-Based Virtual Screening: From Classical to Artificial Intelligence. Frontiers in Chemistry. 2020;8: 343.

Manda S, Moudgil M, Mandal SK. Rational drug design. European Journal of Pharmacology. 2009;625(1-3):90-100.

March-Vila E, Pinzi L, Sturm N, Tinivella A, Engkvist O, Chen H, et al. On the Integration of *In Silico* Drug Design Methods for Drug Repurposing. Frontiers in

pharmacology [Internet]. 2017;8:298 [cited 2020 May 08]. Available from URL: https://www.ncbi.nlm.nih.gov/pmc/articles/PMC5440551/

McMullin M, Wilkins B, Harrison C. Management of polycythaemia vera: a critical review of current data. British Journal of Haematology. 2015;172(3):337-349.

Nicolas C, Peineau S, Amici M, Csaba Z, Fafouri A, Javalet C, et al. The JAK/STAT Pathway Is Involved in Synaptic Plasticity. Neuron. 2012 Jan 26;73(2):374-390.

Pantziarka P, Bouche G, Meheus L, Sukhatme V, Sukhatme V.P, Vikas P. The Repurposing Drugs in Oncology (ReDO) Project. Ecancermedicalscience [Internet]. 2014; 8:442 [cited 2020 May 08]. Available from URL: https://www.ncbi.nlm.nih.gov/pmc/articles/PMC4096030/

Passamonti F, Maffioli M. The role of JAK2 inhibitors in MPNs 7 years after approval. Blood. 2018;131(22):2426-2435.

Pettersen E, Goddard T, Huang C, Couch G, Greenblatt D, Meng E, et al. UCSF Chimera--A visualization system for exploratory research and analysis. Journal of Computational Chemistry. 2004;25(13):1605-1612.

Sieveen KS, Sikka S, Surana R, Dai X, Zhang J, Kumar AP, et al. Targeting the STAT3 signaling pathway in cancer: Role of synthetic and natural inhibitors. Biochimica et Biophysica Acta (BBA) - Reviews on Cancer. 2014;1845(2):136-154.

Smyth M S, Martin J H J. x Ray crystallography. Journal of Clinical Pathology. 2000; 53(1):8-14.

Spivak JL. Myeloproliferative Neoplasms. New England Journal of Medicine. 2017;376(22):2168-2181.

Strober BE, Menon K. Folate supplementation during methotrexate therapy for patients with psoriasis. Journal of the American Academy of Dermatology. 2005; 53(4):652-659.

Tefferi A, Vannucchi AM, Barbui T. Polycythemia vera treatment algorithm 2018. Blood Cancer Journal [Internet]. 2018; 8(1) [cited 2020 May 09]. Available from URL: https://www.nature.com/articles/s41408-017-0042-7

Thomas S, Fisher K, Snowden J, Danson S, Brown S, Zeidler M. Methotrexate Is a JAK/STAT Pathway Inhibitor. Public Library of Science [Internet]. 2015;10(7):e0130078 [cited 2020 May 09]. Available from URL: https://journals.plos.org/plosone/article?id=10.1371/journal.pone.0130078

Vannucchi AM. How I treat polycythemia vera. Blood. 2014;124:3212-3220.

Verstovsek S, Bose P. JAK2 inhibitors for myeloproliferative neoplasms: what is next?. Blood. 2017;130:115-125.

Verstovsek S, Talpaz M, Ritchie E, Wadleigh M, Odenike O, Jamieson C, et al. A phase I, open-label, dose-escalation, multicenter study of the JAK2 inhibitor NS-018 in patients with myelofibrosis. Leukemia. 2017; 31:393-402.

Wade R, Rose M, Neilson AR, Stirk L, Rodriguez-Lopez R, Bowen D, et al. Ruxolitinib for the treatment of myelofibrosis: a NICE single technology appraisal. Pharmacoeconomics. 2013;31(10):841-852.

Wang R, Gao Y, Lai L. LigBuilder: A Multi-Purpose Program for Structure-Based Drug Design. Journal of Molecular Modeling. 2000; 6: 498-516.

Wang R, Lai L, Wang S. Further development and validation of empirical scoring functions for structure-based binding affinity prediction. Journal of Computer-Aided Molecular Design. 2002;16:11-26.

Weinblatt ME. Methotrexate in Rheumatoid Arthritis: A Quarter Century of Development. Transactions of the American Clinical and Climatological Association. 2013;124:16-25.

Weinstein GD. Methotrexate. Annals of Internal Medicine. 1977;86(2):199-204.

Williams N, Bamert R, Patel O, Wang C, Walden P, Wilks A, et al. Dissecting Specificity in the Janus Kinases: The Structures of JAK-Specific Inhibitors Complexed to the JAK1 and JAK2 Protein Tyrosine Kinase Domains. Journal of Molecular Biology. 2009;387(1):219-232.

Wolber G, Langer T. LigandScout: 3-D Pharmacophores Derived from Protein-Bound Ligands and Their Use as Virtual Screening Filters. Journal of Chemical Information and Modeling. 2005;45(1):160-169.

Zhang XN, Meng JX, Luan CL, Chen JF, Tang G, He ZY, et al. Relationship of JAK2V617F gene mutation with cell proliferation and coagulation function in myeloproliferative neoplasms. Journal of Hainan Medical University. 2017; 23(10): 135-137.

List of Publications and Abstracts

The following abstract was submitted to the:

- 9th Annual International Conference on Pharmaceutical Sciences 2-5 May 2022, Athens, Greece
- Mini-Reviews in Medicinal Chemistry Journal

Athens Institute for Education and Research Abstract Submitting Form	
Conference	9th Annual International Conference on Pharmaceutical Sciences, 2-5 May 2022, Athens, Greece
Title of Paper	**Validation of the Repurposing of the Methotrexate Scaffold for the Design of Janus Kinase Modulators with Potential Inhibitory Activity**
For more than one author, please copy and paste the following eight rows for each additional author.	
Title	Ms
First Name	Francesca
Family Name	Borg
Position	Student
University/ Organization	University of Malta
Country	Malta
E-mail	borgfrancesca@hotmail.com
Phone(s)/Fax	+356 79913607
Title	Dr
First Name	Claire
Family Name	Shoemake
Position	Supervisor
University/ Organization	University of Malta
Country	Malta
E-mail	claire.zerafa@um.edu.mt
Phone(s)/Fax	+356 99423449

Abstract

Polycythaemia vera, a rare blood cancer, has been associated with a mutation in the JAK2V617F gene, in turn leading to the activation of the JAK/STAT signalling pathway. This receptor is therefore a target in the identification of molecules that target myeloproliferative neoplasms. Antagonism can reverse underlying marrow pathology, disrupting erythrocytosis and other inflammatory responses. The identification of low-dose methotrexate as a selective and potent JAK2 antagonist indicates that there is potential for its repurposing, since current treatments are associated with the increased risk of transformation of polycythaemia vera to acute leukemia. This study uses the methotrexate scaffold as the lead molecule in order to identify high affinity ligands using two different approaches: virtual screening and de novo design. Conformational analysis was performed on the methotrexate scaffold. The methotrexate molecule was modelled and docked into the apo JAK2 receptor. This process generated 20 different conformers. The optimal conformer was identified by calculating the ligand binding energy in kcalmol-1 and the ligand binding affinity in pKd for each conformer and plotting them on a line graph. The molecule that was the most energetically feasible and that had the highest affinity was chosen as the best optimal conformer. In the Virtual Screening approach, the methotrexate molecule was used as the template to generate a cohort of Lipinski Rule compliant hit molecules. These hits were docked into a generated protomol and the resultant 991 compliant molecules were ranked according to their affinity for the JAK2 ligand binding pocket. In the de novo approach 3 seed structures were modelled, based on the optimal methotrexate molecule and growth was allowed, through a fragmentation exercise, within the pharmacophoric space, in order to generate novel molecules. A number of filters were applied to ensure that the best molecules are Lipinski Rule compliant, and hence able to penetrate the blood brain barrier. Lipinski Rule compliant de novo molecules were generated and separated into different families based on their pharmacophoric similarities, and then ranked according to affinity. The optimal molecules obtained from these two approaches will be retained for further validation and optimization.

Keywords (at least three)	Methotrexate, JAK2 receptor, Polycythemia Vera

Please email to: atiner@atiner.gr as an attached file or fax it to +30 210 3634209

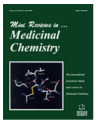

Mini-Reviews in Medicinal Chemistry

(Mini-Reviews in Medicinal Chemistry)
ISSN (Print): (1389-5575)
ISSN (Online): (1875-5607)

Contact Information

First Name: Francesca

Last Name: Borg

Email address: francesca.borg.16@um.edu.mt

Password: ••••••

Abstract Information

Title: Validation of the Repurposing of the Methotrexate Scaffold for the Design of Janus Kinase Modulators with Potential Inhibitory Activity

Abstract: Polycythaemia vera, a rare blood cancer, has been associated with a mutation in the JAK2V617F gene, in turn leading to the activation of the JAK/STAT signalling pathway. This receptor is therefore a target in the identification of molecules that target myeloproliferative neoplasms. Antagonism can reverse underlying marrow pathologies, disrupting erythrocytosis and other inflammatory responses. The identification of low-dose methotrexate as a selective and potent JAK2 antagonist indicates that there is potential for its repurposing, since current treatments are associated with the increased risk of transformation of polycythaemia vera to acute leukemia. This study uses the methotrexate scaffold as the lead molecule in order to identify high affinity ligands using two different approaches: virtual screening and de novo design. Conformational analysis was performed on the methotrexate scaffold. The methotrexate molecule was modelled and docked into the apo JAK2 receptor. This process generated 20 different conformers. The optimal conformer was identified by calculating the ligand binding energy in kcalmol-1 and the ligand binding affinity in pKd for each conformer and plotting them on a line graph. The molecule that was the most energetically feasible and that had the highest affinity was chosen as the best optimal conformer. In the Virtual Screening approach, the methotrexate molecule was used as the template to generate a cohort of Lipinski Rule compliant hit molecules. These hits were docked into a generated protomol and the resultant 991 compliant molecules were ranked according to their affinity for the JAK2 ligand binding pocket. In the de novo approach 3 seed structures were modelled, based on the optimal methotrexate molecule and growth was allowed, through a fragmentation exercise, within the pharmacophoric space, in order to generate novel molecules. A number of filters were applied to ensure that the best molecules are Lipinski Rule compliant, and hence able to penetrate the blood brain barrier. Lipinski Rule compliant de novo molecules were generated and separated into different families based on their pharmacophoric similarities, and then ranked according to affinity. The optimal molecules obtained from these two approaches will be retained for further validation and optimization.

keywords: JAK2 | Methotrexate | Polycythaemia Vera | Myeloproliferative Neoplasms | Drug Repurposing | Medicinal Chemistry

Add Author Information

First Name *	Francesca	**Institution ***	University of Malta
Last Name *	Borg	**Department ***	Department of Pharmacy
Email Address *	francesca.borg.16@um.edu.mt	**Address**	
Field of Expertise *	Medicinal Chemistry	**Country ***	Malta
City *	Sigġiewi	**Phone**	

Upload Abstract File

Upload Abstract File: Browse | Francesca Borg Abstract.pdf

Note: Only pdf docx & doc file type is allowed.

Verify Captcha: I'm not a robot

Submit Abstract

Appendix I

Ethics Approval

30/08/2021 University of Malta Mail - FRECMDS_2021_180 - ID :-9559_24082021_Francesca Borg

L-Università ta' Malta

Francesca Borg <francesca.borg.16@um.edu.mt>

FRECMDS_2021_180 - ID :-9559_24082021_Francesca Borg

FACULTY RESEARCH ETHICS COMMITTEE <research-ethics.ms@um.edu.mt> 30 August 2021 at 11:28
To: Francesca Borg <francesca.borg.16@um.edu.mt>
Cc: "Dr. Claire Shoemake" <drclaireshoemake@gmail.com>

Dear Ms Borg,

Since your self-assessment resulted in no issues being identified, FREC will file your application for record and audit purposes but will not review it.

Any ethical and legal issues including data protection issues are your responsibility and that of the supervisor.

Good luck with your project!

Regards,
Annalise
[Quoted text hidden]
[Quoted text hidden]

Addendum

A CD containing all the relevant raw data used in this project includes:

- A table containing the 3D structures, ligand binding affinities and ligand binding energies of the 20 conformers of methotrexate
- A word document containing the ligand binding energies of the 20 conformers of methotrexate extracted from X-Score® v1.3 (Wang et al,2002)
- An index file from all the seeds of the *de novo* results extracted from LigBuilder® v1.2 (Wang et al, 2000)